



Catalysts for upgrading solvent refined lignite
by Nam Kyun Kim

A thesis submitted in partial fulfillment of the requirements for the degree of Doctor of Philosophy in
Chemical Engineering
Montana State University
© Copyright by Nam Kyun Kim (1982)

Abstract:

The solvent refined lignite (SRL), made at the University of North Dakota Process Development Unit, was a solid having a nominal melting point of 160°C. The SRL was pulverized and mixed with a donor solvent, tetralin. The SRL to tetralin ratio of 1:1 was selected to pretreat in a high pressure and temperature reactor. The optimized reactor conditions were a reaction temperature of 475°C, an initial hydrogen pressure of 2000 psig and a retention time of 40 minutes. Under these conditions approximately 97% of the SRL was dissolved in tetralin. The resulting solution was used to test the 27 developmental catalysts.

The catalysts were developed by impregnating on the γ -alumina the 3 active metals; MoO₃, CoO, and WO₃, each at 3 levels. The effect of these factors on upgrading of the SRL was evaluated in terms of denitrogenation, desulfurization, and hydrocracking. The multiple linear regression analysis showed that the metal compositions for the best overall catalytic performance were 9.5% MoO₃, 4.3% CoO, and 4% WO₃ (% of carrier weight).

A model was developed based on the results of scanning electron micrographs to explain some of the physical characteristics of the catalysts. The disadvantage of the incipient wetness method used in metal impregnation was explained, and the preferable pore structure and distribution were suggested.

CATALYSTS FOR UPGRADING SOLVENT REFINED LIGNITE

by

Nam Kyun Kim

A thesis submitted in partial fulfillment
of the requirements for the degree

of

Doctor of Philosophy

in

Chemical Engineering

MONTANA STATE UNIVERSITY
Bozeman, Montana

October 1982

D378
K56135
cop.2

APPROVAL

of a thesis submitted by

Nam Kyun Kim

This thesis has been read by each member of the thesis committee and has been found to be satisfactory regarding content, English usage, format, citations, bibliographic style, and consistency, and is ready for submission to the College of Graduate Studies.

November 9, 1982
Date

Lloyd Berg
Chairperson, Graduate Committee

Approved for the Major Department

November 9, 1982
Date

John T. Sears
Head, Major Department

Approved for the College of Graduate Studies

11-11-82
Date

W. D. Malone
Graduate Dean

STATEMENT OF PERMISSION TO USE

In presenting this thesis in partial fulfillment of the requirements for a doctoral degree at Montana State University, I agree that the Library shall make it available to borrowers under rules of the Library. I further agree that copying of this thesis is allowable only for scholarly purposes, consistent with "fair use" as prescribed in the U.S. Copyright Law. Requests for extensive copying or reproduction of this thesis should be referred to University Microfilms International, 300 North Zeeb Road, Ann Arbor, Michigan 48106, to whom I have granted "the exclusive right to reproduce and distribute copies of the dissertation in and from microfilm and the right to reproduce and distribute any abstract in any format."

Signature

Nam K. Kim

Date

Oct. 22, 82

ACKNOWLEDGMENT

The author would like to thank the Department of Energy and Associated Western Universities, Inc. for the financial support that made this research possible. Special thanks are given to Dr. Lloyd Berg, director of this research, and Dr. F. P. McCandless for their guidance. The moral support and encouragement of the staff of the Chemical Engineering Department are gratefully acknowledged.

Appreciation is extended to Lyman Fellows for his fabrication of the research equipment, Ms. Alice Brekke for proofreading, Andy Brixt for the preparation of SEM, Dr. E. Abbott for the NMR, and Mrs. M. C. Wagner of Katalco for the analyses of surface areas and pore distribution. A special thanks goes to Dr. R. Lund, who helped with the statistical design.

Finally, I wish to express my gratitude to my wife, Sook, son, Daniel (9), and daughter, Nancy (7). Without their encouragement and patience, I could never have been a graduate student.

TABLE OF CONTENTS

	Page
APPROVAL PAGE	ii
STATEMENT OF PERMISSION TO USE	iii
ACKNOWLEDGMENT	iv
TABLE OF CONTENTS	v
LIST OF TABLES	vii
LIST OF FIGURES	viii
ABSTRACT	xi
INTRODUCTION	1
BACKGROUND	3
Lignite	5
Solvent Refined Lignite	5
Chemical Structure of Lignite	10
Liquefied Lignite	12
Catalytic Upgrading	15
Catalyst	17
Trickle Bed Reactor	20
Research Objective	20
EXPERIMENTAL	22
Feedstock	22
Preparation of Catalysts	24
Continuous Trickle Bed Reactor	30
Operation of Continuous Trickle Bed Reactor	32
Analytical Procedure	33
RESULTS AND DISCUSSION	34
Preparation of Feed Solution	34
Performance Tests	46
Effect of Metal Compositions on Upgrading	50
Development of A Model for Catalyst	75

	Page
SUMMARY AND CONCLUSIONS	92
RECOMMENDATION FOR FUTURE STUDY	94
LITERATURE CITED	95
APPENDICES	100
A. Surface Area and Pore Distribution of Catalyst Carriers	101
B. Sample Calculation of Pore Volumes	119
C. ASTM D-86 Distillation Data	123
D. Modeling of Katalco Carrier	127

LIST OF TABLES

Table	Page
I. Composition and Characteristics of Feed and Products.....	9
II. Analyses of SRL and North Dakota Lignites.....	23
III. Analysis of Ash.....	24
IV. Systematic Preparation of 27 Catalysts.....	26
V. Summary of the First 15 Batch Runs.....	35
VI. Effect of Water Addition on Catalytic Performance.....	37
VII. SRL Dissolubility at Various Operating Conditions.....	40
VIII. SRL Dissolubility at Extended Operating Conditions.....	42
IX. Catalytic Performances: KT-14 vs. Blank Carrier.....	47
X. Nitrogen Removal With KT Series Catalysts.....	49
XI. Summary of Catalytic Performance.....	52
XII. Analysis of Variance for Three Factors at Three Levels.....	60
XIII. Multiple Regression Analysis for Denitrogenation.....	61
XIV. Analysis of Variance for Desulfurization as Response Variables.....	70
XV. Multiple Regression Analysis for Desulfurization.....	71
XVI. Multiple Regression Analysis for Gasoline Yield.....	76
XVII. Multiple Regression Analysis for Heavy Oil Yield.....	77
XVIII. Comparison of Various Catalysts.....	83
XIX. Pore Volume and Surface Area Following 10% MoO ₃ , 4% CoO, and 8% WO ₃ Impregnation on Katalco Carrier.....	85
XX. Pore Volume and Surface Area Following 10% MoO ₃ , 4% CoO, and 8% WO ₃ Impregnation on Nalco A Carrier.....	86

LIST OF FIGURES

Figure	Page
1. Coal fields in the Northern Great Plains province	4
2. Schematic flow diagram for 50 lb/hr PDU with mass rates and run conditions.	8
3. Chemical precursors of coal.	11
4. Representative partial structures of coal	13
5. Comparison of lignite with other sources of hydrocarbon.	14
6. A theoretical molecule and thermal breakup of coal (Wiser)	16
7. Approximate reaction routines for the HDS, HDN, and HDO from five membered heterorings in the presence of catalyst.	18
8. A 3-D representation of 3 ³ experimental design	27
9. Electric furnace and auxiliary equipment for sulfidation of catalyst.	29
10. Trickle bed reactor arrangement	31
11. Effect of water addition in wt% denitrogenation and wt% desulfurization	38
12. Effect of reactor temperature and retention time at two levels of hydrogen pressure on SRL dissolubility in tetralin	41
13. Effect of reactor temperature on SRL dissolubility in tetralin at two levels of retention time.	44
14. Effect of hydrogen pressure on SRL dissolubility at two different temperature levels	45
15. Effect of retention time on SRL dissolubility in tetralin at 475°C and 2000 psig of H ₂	45
16. Catalytic performance of KT-14 against blank base in denitrogenation	48
17. ASTM D-86 distillation, feed and 8-hr composite product of blank carrier	51

Figure	Page
18. Catalytic performance in denitrogenation as a function of MoO_3 concentration	54
19. Catalytic performance in denitrogenation as a function of CoO , WO_3 , and MoO_3 concentrations	55
20. Catalytic performance in denitrogenation as a function of CoO concentration	56
21. Catalytic performance in denitrogenation as a function of MoO_3 , WO_3 , and CoO concentrations	57
22. Catalytic performance in denitrogenation as a function of WO_3 concentration	58
23. Catalytic performance in denitrogenation as a function of MoO_3 , CoO , and WO_3 concentrations	59
24. Catalytic performance in desulfurization as a function of MoO_3 concentration	63
25. Catalytic performance in desulfurization as a function of CoO , WO_3 , and MoO_3 concentrations	64
26. Catalytic performance in desulfurization as a function of CoO concentration	65
27. Catalytic performance in desulfurization as a function of MoO_3 , WO_3 , and CoO concentrations	66
28. Catalytic performance in desulfurization as a function of WO_3 concentration	67
29. Catalytic performances in desulfurization as a function of MoO_3 , CoO , and WO_3 concentrations	68
30. Catalytic performance in hydrocracking as a function of CoO , WO_3 , and MoO_3 concentrations	72
31. Catalytic performance in hydrocracking as a function of MoO_3 , WO_3 , and CoO concentrations	73
32. Catalytic performance in hydrocracking as a function of MoO_3 , CoO , and WO_3 concentrations	74

Figure	Page
33. Scanning electron photomicrographs of various catalysts:	
(A) Katalco blank carrier	78
(B) KT-14 with 10% MoO ₃ , 4% CoO, and 8% WO ₃ on Katalco carrier	78
(C) KT-14 after 8-hr run	78
(D) Union Carbide Linde 13X with 10% MoO ₃ , 4% CoO, and 8% WO ₃	79
(E) Ketjen LA-3P with 10% MoO ₃ , 4% CoO, and 8% WO ₃	79
(F) Nalco A with 10% MoO ₃ , 4% CoO, and 8% WO ₃	80
(G) Harshaw CoMo 0401 with 9% MoO ₃ and 3% CoO	80
34. Three dimensional arrangement of basic granules for Katalco carrier	81
35. Effect of catalyst pore diameter on denitrogenation	84
36. Surface area distribution vs. pore diameter	88
37. Distribution of MoO ₃ vs. pore diameter	89
38. Representative structures of pore	90

ABSTRACT

The solvent refined lignite (SRL), made at the University of North Dakota Process Development Unit, was a solid having a nominal melting point of 160°C. The SRL was pulverized and mixed with a donor solvent, tetralin. The SRL to tetralin ratio of 1:1 was selected to pretreat in a high pressure and temperature reactor. The optimized reactor conditions were a reaction temperature of 475°C, an initial hydrogen pressure of 2000 psig and a retention time of 40 minutes. Under these conditions approximately 97% of the SRL was dissolved in tetralin. The resulting solution was used to test the 27 developmental catalysts.

The catalysts were developed by impregnating on the γ -alumina the 3 active metals; MoO_3 , CoO , and WO_3 , each at 3 levels. The effect of these factors on upgrading of the SRL was evaluated in terms of denitrogenation, desulfurization, and hydrocracking. The multiple linear regression analysis showed that the metal compositions for the best overall catalytic performance were 9.5% MoO_3 , 4.3% CoO , and 4% WO_3 (% of carrier weight).

A model was developed based on the results of scanning electron micrographs to explain some of the physical characteristics of the catalysts. The disadvantage of the incipient wetness method used in metal impregnation was explained, and the preferable pore structure and distribution were suggested.

INTRODUCTION

Currently the United States consumes close to 80 quadrillion Btu (quads) per year, importing increasing amounts of oil to meet its needs. The United States by 1978 already imported almost 8.5 million barrels of oil per day—over 17 quadrillion Btu per year. It is generally recognized that this level of imports is unhealthy for the U.S. economy. Every worker in the United States consumes 1.55 billion Btu per year for all purposes of employment [1]. If employment is to continue to grow, energy will have to be supplied to the society in increasing amounts from coal. Production of oil and natural gas is declining at an annual rate of about 4 to 5%. Nearly 45% of the petroleum that is currently produced has been obtained by water flooding and other secondary recovery techniques applied to mature fields [2].

In the present United States environment of decreasing availability of petroleum and natural gas, coal is a natural candidate for the raw material for liquids and gases. The reasons for this are that the United States has more energy available in the form of coal than in the combined sources of petroleum, natural gas, oilshale, and tar sands. The use of coal for energy will certainly increase in the United States during the next several decades. Utilization of domestically abundant coal, both for the production of power and as a feedstock in synthetic fuels production, will require processing operations on a large commercial scale [3].

The transportation sector demands exclusively liquid fuels, the residential and commercial sectors depend heavily on gaseous fuels, and three quarters of the energy used by industry are constituted as liquid and gaseous fuels [2]. Consequently, the conversion of

coal to gaseous and liquid fuels in commercial quantities is vital to ensuring the availability of fuel in conventional forms for the major users.

Coal gasification and liquefaction processes were pioneered during the 1920s and 1930s in Germany. They constitute the basis for much of today's technology. The accomplishment of Friederich Bergius [4] brought him the Nobel Prize for chemistry in 1931. His direct hydrogenation of coal at elevated temperature (430°C or 806°F) and pressures (3,000-10,000 psig) led to the production of gasoline and aviation fuel. At the same time Mathias Pier and co-workers found sulfur resistant, coal-hydrogenation catalysts that reduced the severity of the environment for liquefaction while improving conversion efficiency. The production of synthetic fuels from coal will have justification due to the convenience of using liquids and gases and due to the ways in which transportation and domestic systems have been developed [5].

BACKGROUND

The United States Geological Survey estimated that the lignite shares 6% of the demonstrated coal reserve base (437 billion tons). The lignite in the Northern Great Plains (NGP) occurs in relatively thick seams ranging from 5 ft to more than 100 ft and typically with overburden from 50 to 200 ft. The ratio of "overburden volume to lignite volume" is most favorable when compared with that of higher ranking coal [6].

Most significant is the fact that the NGP surface mineable reserve base totals 82.3 billion tons or 58% of the national surface mineable reserve base. More than 95% of these resources are lignite and subbituminous (classified as low rank coals) occurring in the Fort Union and Powder River Regions and the Bull Mountain Field (Figure 1).

Nearly 100% of NGP coal mined since the 1960s has been used to generate electricity, but the future potential for the production of synthetic fuels and chemicals is increasing. Since 1971, plans for construction of seventeen separate mine-mouth coal synfuel plants in the NGP have been announced. These plans include eight separate gasification plants, nine liquefaction plants, and two in-situ gasification pilot operations [7].

The first commercial scale synthetic fuels project, the Great Plains Gasification Plant (GPGP) of Oliver County, North Dakota, has already begun on July 25, 1980 and is scheduled for full gas production by the end of 1984 [8]. Project Lignite, equivalent to the SRC-I, was awarded to the University of North Dakota in 1972 for the purpose of determining the appropriate technological approach to the conversion of lignite to clean fuel. The original plan was expected to extend the two stage conversion of lignite to liquid fuel (equivalent to the SRC-II) with the solvent refined lignite (SRL) as an intermediate solid fuel. The first stage to convert lignite to the SRL has been successfully accomplished,

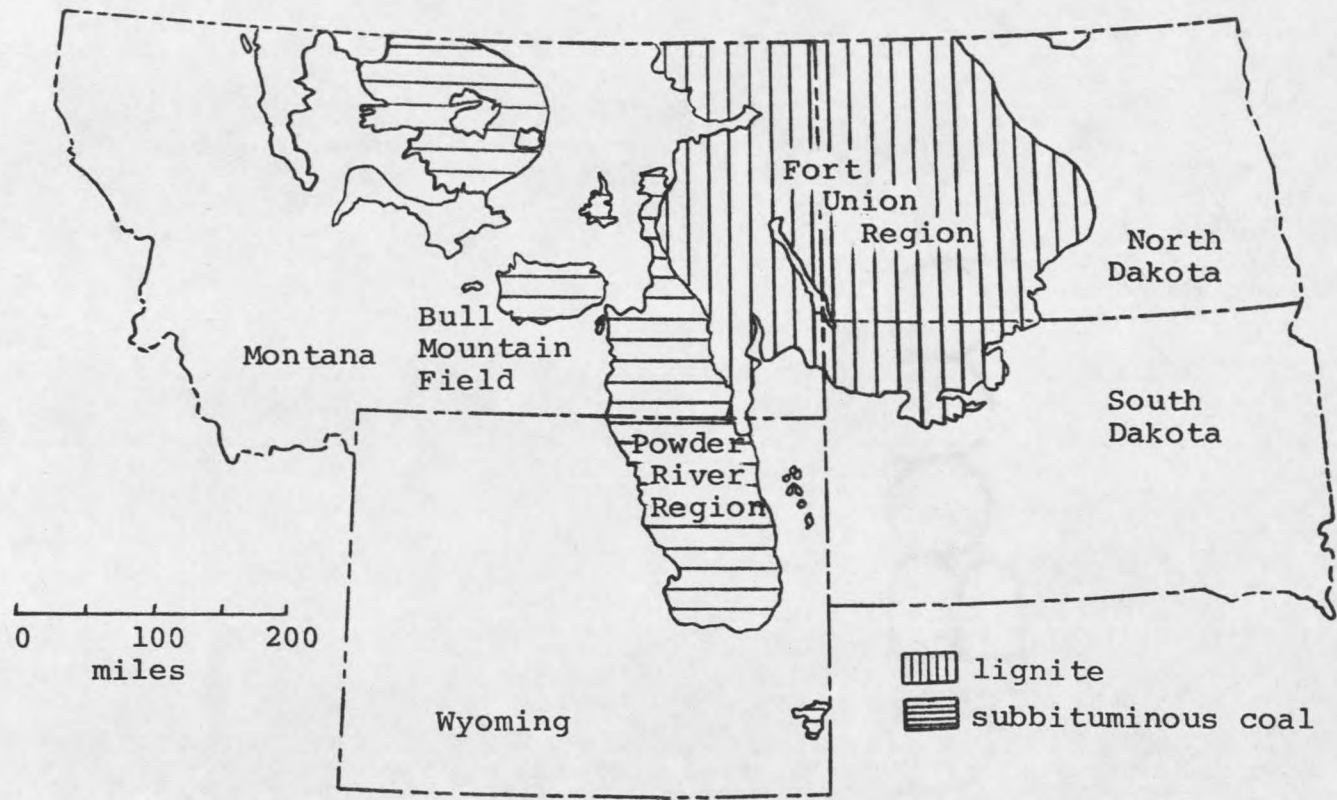


Figure 1. Coal fields in the Northern Great Plains province.

but the second stage that catalytically hydrotreats the SRL to the distillate fuel was not implemented [9].

The objective of this research is to catalytically upgrade the SRL to liquid fuel for immediate industrial use or to clean distillate suitable for conventional refinery feedstock.

Lignite

Lignite is a brownish-black coal that is intermediate in coalification between peat and subbituminous coal. According to the classification system adopted by the American Society for Testing and Materials (ASTM), the lignite is the lowest rank of coals in terms of calorific value (less than 8300 Btu per pound on a moisture, mineral-matter-free basis) and carbonaceous content (47 to 59%) [10].

While the use of lignite to generate electricity will predominate other uses, a strong potential also exists for the conversion of lignite to synthetic fuels. The Great Plains Gasification Plant is designed to convert the North Dakota lignite into pipeline quality synthetic natural gas (SNG) having about 977 Btu per standard cubic foot (scf). Approximately 137 million scf per day of SNG and other byproducts such as anhydrous ammonia, tar, oil, phenols, and naphtha will be produced by processing 22,000 tons per day of lignite. Lignite displays unique properties: (1) its high reactivity evidenced by spontaneous combustion, (2) non-coking and non-swelling nature with high permeability upon heating, and (3) excellent sulfur absorbent qualities [6].

Solvent Refined Lignite

The Project Lignite Process Development Unit [11] has a normal design capacity of 50 pounds of lignite feed per hour and produces light liquids and gases in addition to approximately 15 pounds per hour of SRL having a melting point of 150 to 205°C (300 to 400°F).

Lignite as received is pulverized to slurry with solvent. The slurry is pressurized, preheated and reacted at a selected temperature (normally at 434°C or 814°F) and pressure (2500 psig) in a reducing gas environment. The products are then separated as gases, liquids, and SRL from the unreacted coal and mineral matters. The flow rate of solvent to the slurry mixing tank is controlled by the signals from an orifice in the solvent feed line. The flow out of the tank is controlled by the slurry level in the tank.

Two dissolvers (or reactors), R-1A and R-1B, are made from 18-ft lengths of 4 7/8-inches OD by 3 7/8-inches ID Incoloy 800 tubing. The inlet of each reactor is at the bottom and the outlet at the top, with another outlet at the center. Thus any multiple of 10 ft lengths up to 40 ft can be assembled. Consequently, residence times for the slurry can be varied four-fold at a constant feed rate.

The gas-slurry mixture then goes to a series of separators at high, intermediate, and low pressures. The vapor products consist primarily of unreacted carbon monoxide and hydrogen, carbon dioxide, hydrogen sulfide, ammonia and light hydrocarbons.

The liquid products consist mainly of water, process solvent, and lighter products. Light end column F-2 is operated at 10 to 15 psig. The overhead product is light oil, essentially a stabilized naphtha, consisting of hydrocarbons ranging from about C₅ to perhaps as high as 350°F to 450°F boiling point. The bottom product is recycled to the slurry mix tank.

Mineral separation consists of a system of vessels and pumps designed for the high temperature extraction of solvent refined lignite plus solvent from the mineral matter and unconverted lignite using toluene as a diluent. The toluene-slurry mixture is then fed to the vacuum flash drum F-1 via the settling tower V-8 (18 inch diameter by 12 ft high) in which the terminal velocity of the settling particles is greater than fluidizing solvent (toluene) and SRL velocity.

The bottoms from the toluene flash vessel V-9 is fed through preheater E-11 and into the vacuum flash drum F-1. The bottoms from F-1 is the SRL product.

A typical PDU operation is shown in a flow schematic for Run M-33C (Figure 2). In this run, 47 lb/hr of average 36.7% moisture lignite was processed with 407 scf/hr of gas containing 50% H₂ and 50% CO, 91 lb/hr of recycle in the liquid-solid separation system. The rough material balance is shown, as well as pressures and temperatures in the important vessels. The 100 lb of moisture and ash free (MAF) lignite produced 57.4 lb of SRL and light organic liquids, consuming 7.8 lb of CO, 0.04 lb of H₂, and 2.38 lb of water with a wt % MAF coal conversion of 93.4 [12].

A typical composition and characteristics of SRL product from Zap lignite are shown in Table I. Generally it has been customary to classify the quality of the coal products in terms of solubility classes. Oils are hexane soluble fractions, while asphaltenes are terms used for benzene or toluene soluble materials. The benzene insoluble material is preasphaltene (some prefer the term asphaltols or polar compounds) which are soluble in pyridine. The primary product of coal is pyridine soluble, but benzene insoluble. This fraction is subsequently converted to both benzene-soluble and hexane-soluble species through liquefaction process.

Hexane-soluble materials (oils) average about 200-300 in molecular weight. They have little or no functionality. Asphaltenes, on the other hand, are predominantly mono-functional compounds. They consist of phenols and basic nitrogens. Molecular weights range from 300 to 700. Asphaltols have multiple functionality. They consist of polyphenols (up to 5 OH/molecule) and multiple basic nitrogens. Molecular weights range from 400 to 2000 or greater [13]. Conversion in this case is defined as conversion of coal to material soluble in pyridine. This fraction is not found in petroleum and suggests a considerable basic difference between coal and petroleum structure. Low hydrogen content and high

Table I

Composition and Characteristics of Feed and Products

Feed Gas (Project Lignite PDU)

	<u>Vol. %</u>	<u>Wt. %</u>
CO	24.7	81.9
H ₂	75.2	17.8

Material Balance for Gas Components

	<u>Vol% In</u>	<u>Vol% Out</u>	<u>lb/hr In</u>	<u>lb/hr Out</u>
H ₂	75.2	66.2	2.13	1.87
CO	24.7	14.4	9.78	5.81
CO ₂	-	13.2	-	9.91
H ₂ S	-	0.2	-	0.18
CH ₄	-	4.5	-	1.11
C ₂ H ₆	-	1.1	-	0.58
C ₃ H ₈	-	0.3	-	0.33
NH ₃	-	0.1	-	0.04

Ultimate Analysis of Materials

	<u>Lignite Charged</u>	<u>Starting Solvent</u>	<u>Recycle Solvent</u>	<u>Vacuum Bottoms</u>	<u>Deashed SRL</u>
C	45.22	89.03	83.60	80.20	87.42
H	6.43	8.11	9.14	5.20	5.67
N	0.64	0.12	0.20	0.98	1.07
S	0.45	2.23	1.09	0.90	0.98
O*	41.45	0.51	5.97	4.46	4.86
Ash	5.81	0.0	0.0	8.26	0.0

* By difference

Properties of Product SRL

	<u>Measured*</u>	<u>Calculated</u>
Gradient Bar Melting Point, F	327	-
Pyridine Solubles, wt% ash-free	83.5	100
Specific Gravity	1.28	1.25
Heat of Combustion, Btu/lb	14,330	15,990

* F-1 vacuum bottoms

Lignite: North American Coal Co., Zap, N.D.
 Screen size 90%-200 mesh, 100%-60 mesh
 Moisture 31.5%

heteroatom content, compared to petroleum, make coal somewhat intractable with conventional refining technology.

The solvent-refining process consists mainly of conversion of insoluble coal to the pyridine-soluble, toluene-insoluble fraction of SRL. The net result is an increase in aromaticity and some bond breakage, loss of about 20% of the original carbon as gases and volatile liquids, and possible reduction of oxygen, nitrogen, and sulfur.

Chemical Structure of Lignite

It is generally agreed that coal may originate primarily from plants. Through a sequence of evolutionary changes the primary products of the original decomposed plant materials become transformed. The first product is humic acid. Then, the humic acid is transformed eventually into peat, lignite, subbituminous coal, bituminous coal, and finally anthracite [14].

The United States coals consist of primarily vitrinite, usually 80% or more. The composition of this vitrinite is believed to be the result of the coalification of either cellulose or lignin structures, which constitute the majority of the plant components [15]. Some of the chemical precursors of coal are shown in Figure 3.

Lignite is considered to be a crosslinked amorphous polymer, with mostly monoaromatic aggregates connected by relatively weak cross-links. Generally there have been two approaches to deducing chemical structure. One way is to break down the coal material into recognizable fragments and then put them back into an original structure. An alternative approach is direct characterization of solid coal with the use of sophisticated instruments such as IR spectroscopy, NMR spectroscopy and X-ray diffraction. These modern techniques are also severely handicapped because coal is not crystalline and insoluble.

These advanced techniques such as X-ray scattering have been used in the past and conflicting interpretations as to the predominant structure of coal have been reported.

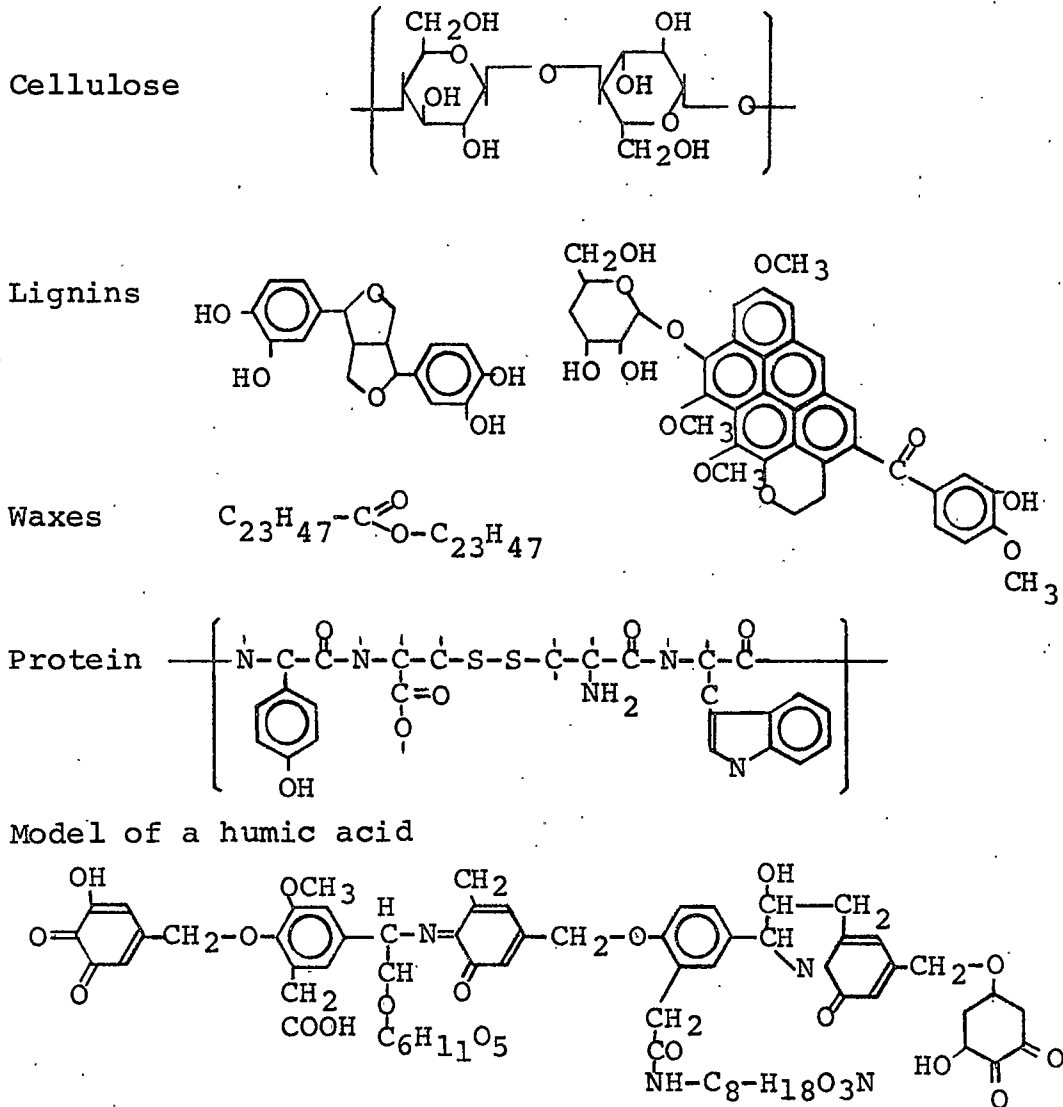


Figure 3. Chemical precursors of coal.

New instruments have evolved recently that are capable of direct characterization in its solid form. The most promising of these tools is a solid state CP-C¹³ NMR developed by Pines [16].

Wender indicated that the carbon skeleton of coals can be considered as consisting of hydroaromatic structure with aromaticity increasing from low-rank to high-rank coals. Figure 4 shows some frames of reference for various ranks of coal [17].

Liquefied Lignite

Coal has chronic problems in utilization. It is a solid of non-uniform composition inorganic material and environmentally objectionable elements such as sulfur, nitrogen, mercury, etc. Conversion of lignite to liquids or gases substantially reduces these disadvantages for lignite. The most important chemical change required for this conversion is the addition of hydrogen (hydrogenation). The amount of hydrogen addition determines the quality of the synthetic product. A comparison of some representative fuels illustrates in Figure 5 the scale of hydrogen/carbon mole ratio [14]. Lignite has a lower hydrogen content than that characteristic of premium quality transportation fuels like gasoline and diesel oil. It can be seen that there is a long path necessary in the conversion of lignite to high quality products.

Liquefaction of coals where the liquid products are the main product has been known for many years since the first work by Bergius. Subsequent development of the process of coal liquefaction have led to a variety of process conditions for producing liquids. The term liquid may need to be defined since some products of coal liquefaction are solids at room temperatures. The degree of conversion can be measured by the amount of material soluble in a certain organic solvent [2].

Wiser [18] showed in 1975 a schematic representation of structural groups and connecting bridges in bituminous coal. It may consist of layers of condensed aromatic and

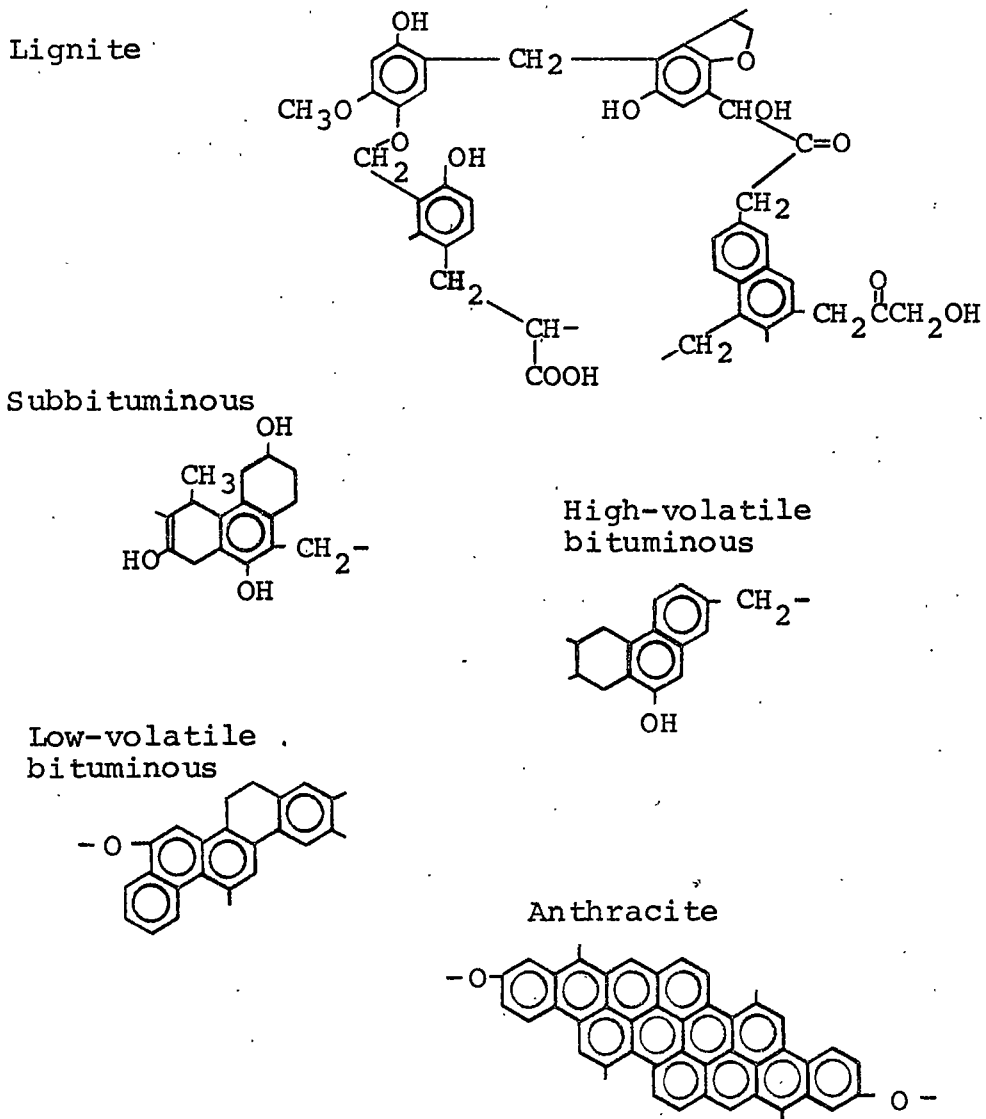


Figure 4. Representative partial structures of coal.

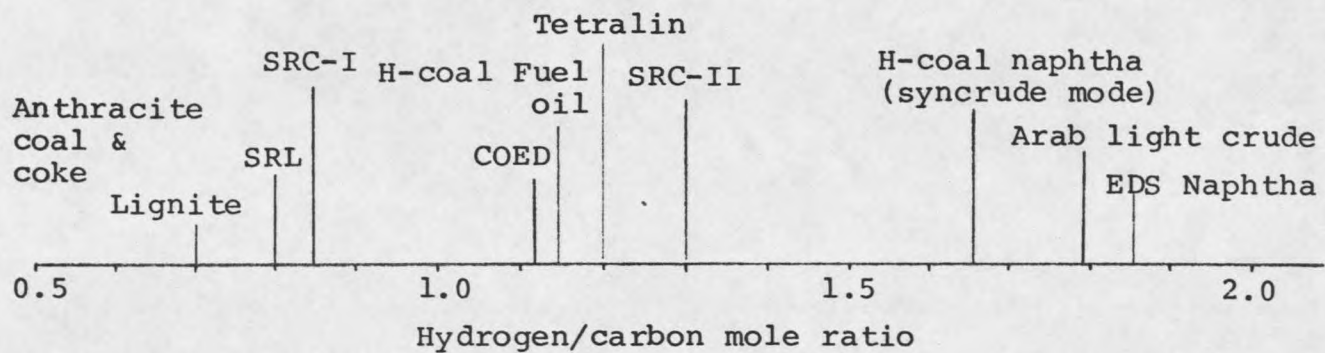
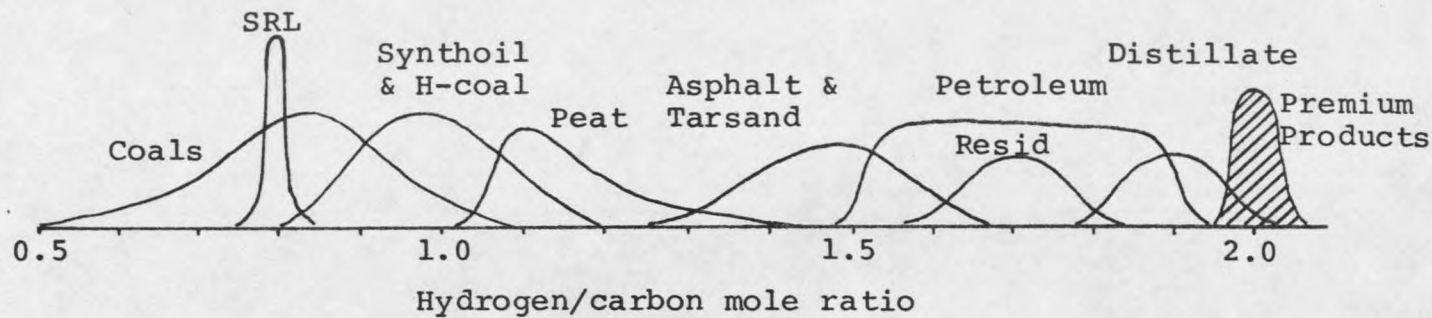


Figure 5. Comparison of lignite with other sources of hydrocarbon.

hydroaromatic clusters ranging in sizes from one to several rings per cluster with an average of three rings per condensed configuration. The significance of these theoretical molecules is the location of a number of relatively weak bonds indicated by arrows which can account for the easy thermal breakup of coal into smaller more soluble fragments (Figure 6).

Catalytic Upgrading

In the process of the hydrogenation of lignite to produce synthetic liquid some removal of heteroatoms (sulfur, nitrogen, and oxygen) is also accomplished. Sulfur and nitrogen contents of lignite are often greater than 1% and oxygen content is sometimes over 20%. Such heteroatoms are responsible for some of the coal conversion and upgrading problems. Upgrading process not only improves the heating value of the fuel but also makes resulting products more environmentally acceptable.

Hydrogenation of liquefied coal is slower than that of petroleum crudes because of the abundance of the polynuclear aromatic compounds. Oxygen is removed primarily as carbon dioxide and water with small amounts of carbon monoxide. About 40-50% of the oxygen and organic sulfur is relatively easy to remove. It is believed to be the result of exchange of OH or carbonyl oxygen by sulfur, due to biological activity in the sediment [19]. The remaining sulfur is much more resistant to removal and is probably present in heterocyclic ring structures.

Removal of S, N, and O from SRL under reducing conditions and in the presence of an industrial catalyst is associated with elimination of hydrogen sulfide, ammonia, and water. Prior to these reactions, C-Y (Y = S, N, or O) bonds may have to be broken, and the fission of one of these bonds may be the rate controlling step [20].

Heterocyclic S, N, and O containing rings are well known for their high resistivity to removal. Ring saturation may be required for N containing compound, while there is some

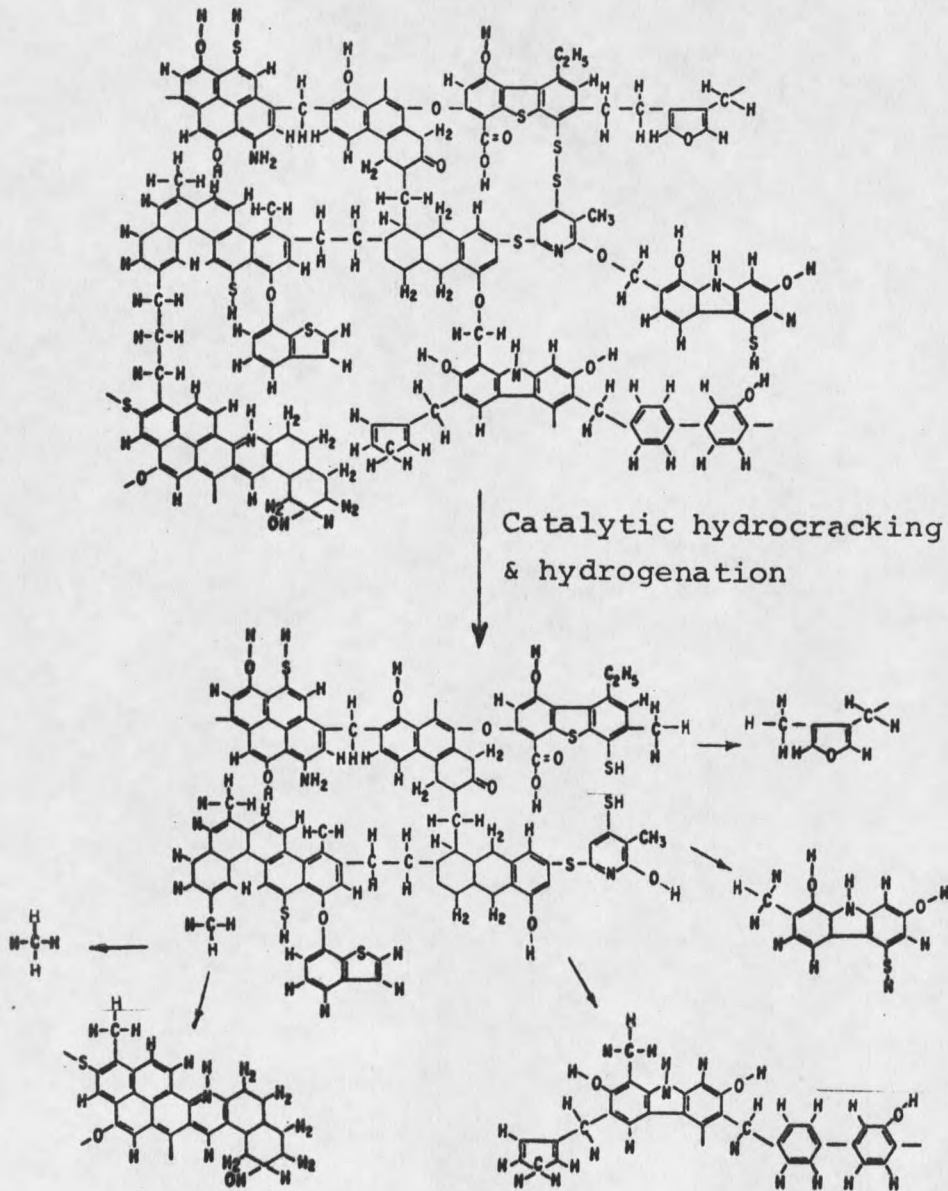


Figure 6. A theoretical molecule and thermal breakup of coal (Wiser).

experimental evidence for the HDS with or without preliminary heteroring hydrogenation [21].

The basic routes for hydrodesulfurization (HDS), hydrodenitrogenation (HDN), and hydrodeoxygenation (HDO) of heterocyclic compounds are shown in Figure 7 as suggested by Furimsky [22]. The hydrogenation of the heteroring is an equilibrium process affected by the concentration of hydrogen [23].

Hydrocracking is extensively practiced commercially in petroleum refining to produce high quality gasoline, jet fuel, diesel, high quality lubricant [24,25,26,27]. Some of the commercially proven catalytic hydrocracking methods are the Standard Oil of Indiana Ultracracking Process and Union Oil Unicracking Process. These processes can tolerate feedstocks with a nitrogen content of as high as 0.3% [28,29].

Under trickle bed catalytic hydrotreating conditions the denitrogenation is always accompanied by other reactions such as hydrogenation, hydrocracking, desulfurization, deoxygenation, coking, and demetallization.

Catalyst

It has long been known that the rates of chemical reactions can be accelerated by small amounts of alien material. Such material is termed a catalyst and it is defined as a substance which increases the rate at which a chemical reaction approaches equilibrium, without being consumed in the process [30]. An appropriate catalyst plays a key role in removing sulfur, nitrogen, and oxygen simultaneously as gaseous hydrogen sulfide, ammonia, and water from the syncrude oil.

The carrier, quite often alumina, refers to a major catalyst constituent that serves as a base or binder for the active metals and promoters. A carrier may be catalytically active or inert. The major function of a carrier is to provide a large surface area so that catalytically active metals can be spread out or dispersed as a monolayer, if possible [31,32,33].

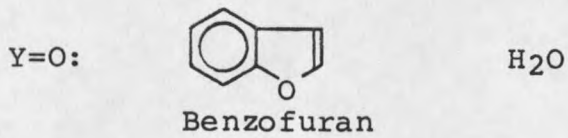
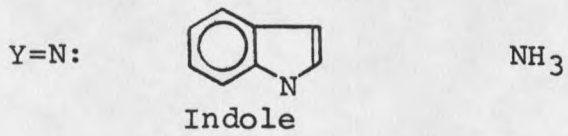
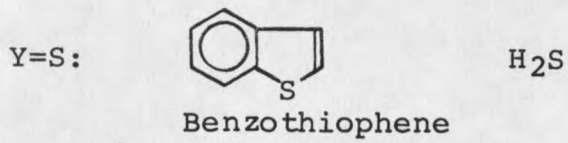
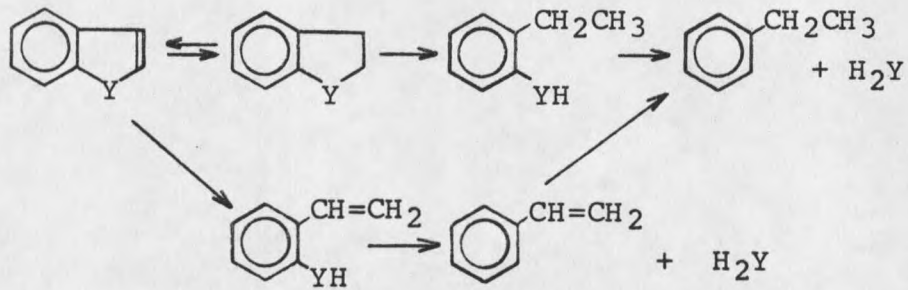


Figure 7. Approximate reaction routines for the HDS, HDN, and HDO from five membered heterorings in the presence of catalyst.

The transition metal oxides and their mixtures with elements of group IV B and V B of the periodic table are of great interest as selective oxidization catalysts [34].

Molybdena and tungstate promoted by cobalt or nickel are well known active agents for their characteristic activities of HDS, HDN, and HDO [35,36]. Activity and selectivity of different catalyst systems were investigated by Qader [37]. Cobalt sulfide on silica (low) alumina was found to be the most active catalyst in the hydrocracking of polycyclic aromatic hydrocarbons. Pelleted tungsten sulfide was the most successful early hydrocracking catalyst [38].

The hydrocracking catalyst has dual functions. They are (1) cracking of high molecular weight hydrocarbons, and (2) hydrogenation of the unsaturates formed either during the cracking step or already present in the feedstock. A balance of hydrogenation and hydrogenolysis activity is vital to maintain catalytic activity [36A]. This balance can be controlled by the appropriate combination of metals and methods of catalyst preparation. Beuther et al. reported that in most commercial applications the molybdenum-cobalt in atomic ratios varies from 0.1:1.0 to 1.0:1.0 but the best activity was observed for ratios around 0.3:1.0 [39].

Popov [40] and Bliznakov et al. [41] demonstrated that a mixture of WO_3 and MoO_3 had a higher activity for oxidation of methanol to formaldehyde than either of the pure oxides.

Effect of silicon dioxide concentration on physicochemical properties of hydrocracking catalyst were investigated by Perezhigina et al. [42]. Addition of SiO_2 to a $CoMoO_4/Al_2O_3$ catalyst increased its cracking and isomerization ability, conversion and rate of iso-to-normal hydrocarbons in the final products. Further, mechanical strength of the catalyst was increased by a factor of 1.5, while a slight decrease of hydrodesulfurization activity was experienced.

Trickle Bed Reactor

The trickle bed reactor is a device in which a liquid phase and a gas phase flow concurrently downward through a packed bed of catalyst material to promote desired reactions. When the fixed bed of catalyst is used with a liquid or mixed liquid plus vapor reactant under operating conditions, the trickle bed reactor is an appropriate choice. Here the liquid reactant is fed at the top of the reactor to distribute evenly over the area of the catalyst bed. Each catalyst particle is wet with the liquid feed as it trickles down through the bed. The reacting gas penetrates the liquid film and reacts on the surface of the catalyst [43].

Use of trickle bed reactor in the petroleum industry involves the processing with hydrogen of various petroleum materials. The HDS, HDN, HDO, and catalytic hydrocracking of heavy or residual oil stock to upgrade the quality has been economically tested using this type of reactor. Ross [44] pointed out that effective distribution of liquid over the catalyst in trickle-phase hydrogenation was the key factor affecting the overall reactor efficiency. The velocity dependence of liquid distribution over the catalyst is a complicated function of the initial distribution, bed-packing arrangement, catalyst particle geometry, wettability of the liquid on the catalyst, local gas velocity, etc. Since the catalyst particles retain a finite amount of liquid both on the external surface and in the pores, the variables that influence the liquid distribution determine its residence time distribution. Therefore, the bench scale trickle phase reactor is suited for the initial product evaluation, rather than the derivation of the reaction kinetics [45].

Research Objective

This research aims to statistically evaluate the effect of the metal concentrations (Mo, W, and Co) on the upgrading of solvent refined lignite (SRL) using Katalco alumina-silica carrier. Upgrading of SRL to liquid fuel for immediate industrial use or to clean distillate

suitable for conventional refinery feedstock includes reduction of nitrogen and sulfur contents and increase in clean products recovered in the ASTM D-86 distillation.

The research plan constitutes three parts. Phase I consists of a pretreatment of SRL to convert it to a manageable liquid feed at room temperature. It includes an optimization of operating conditions for the batch reactor to determine in which conditions SRL promises to make the most dissolution in tetralin. Phase II consists of statistical design of catalysts having three metals, each at three levels. Performance of each catalyst was evaluated in a continuous trickle bed reactor. Phase III consists of the development of a geometric model for the catalyst to explain the physical characteristics and the performance of the catalyst.

EXPERIMENTAL

The SRL was dissolved in a solvent, 1,2,3,4-tetrahydronaphthalene (tetralin), using a batch autoclave with hydrogen at elevated temperatures and pressures. This pretreatment was necessary for preparation of liquid feed, since the SRL as received was a solid. The optimum operating conditions were established for the maximum dissolution of SRL in tetralin and the common feedstock was prepared using these conditions. Twenty-seven catalysts were fabricated using three-factorial design approach. The design is a completely randomized design and the levels of the factor considered are fixed levels. The catalysts were tested in continuous trickle bed reactor to evaluate the performances. The method of chemical analyses is described later in this section.

Feedstock

The SRL was received from the University of North Dakota [45]. A representative analysis of SRL (PDU Run M-33) and the lignite mined near Gascoyne, N.D., is listed in Table II. The SRL is a hard-brittle solid with an incipient melting point of about 90°C at a barometric pressure of 26.5 in. Hg. The SRL was made with 50:50 hydrogen-carbon monoxide syngas at a reactor pressure of 2500 psig and a maximum dissolver temperature of 820°F (438°C).

The X-ray fluorescent analysis of ash is shown in Table III [45]. Ash is the noncombustible mineral matter when lignite is burned under specified conditions of temperature, time, and atmosphere (ASTM D-3174). Any of these constituents may deteriorate the catalytic activity.

Table II

Analyses of SRL and North Dakota Lignites

Quantitative Analysis	Solvent	Zap	SRL from	Gascoyne	SRL from
		Lignite	F-1 bot. (M-39)	Lignite	F-1 bot. (M-33)
	SRL		6.4		2.5
	Coal	64.70	92.3	54.84	97.32
	Ash	6.56	0.28	8.48	0.18
	Water	28.74	1.02	36.68	
	Total	100.00	100.00	100.00	100.00
	Pyridine Solubles		99.72		100.0
Elem. Anal.	Carbon	46.29	87.74	38.28	85.73
	Hydrogen	5.83	6.15	6.83	5.98
	Nitrogen	0.48	0.87	0.51	0.80
	Sulfur	0.29	0.67	0.71	0.94
	Oxygen (by diff.)	40.55	3.55	45.19	6.37
	Ash	6.56	1.02	8.48	0.18
	Total	100.00	100.00	100.00	100.00
Asphal- tene Test	Wt% ash		1.02		0.18
	Wt% unconverted coal		0.28		-
	Wt% preasphaltenes		27.88		21.20
	Wt% asphaltenes		38.34		36.46
	Wt% maltenes & dist. oil		32.48		42.16
	Total		100.00		100.00

Table III

Origin (North Dakota)	Analysis of Ash (Lignites)	
	Wt %	
	Zap	Gascoyne
Loss on ignition (808°C)	0.4	—
SiO ₂	20.2	37.6
Al ₂ O ₃	10.5	5.6
Fe ₂ O ₃	10.0	5.6
TiO ₂	0.5	0.8
P ₂ O ₅	0.6	0.6
CaO	26.7	20.5
MgO	6.8	6.9
Na ₂ O	6.7	4.1
K ₂ O	0.4	0.3
SO ₂	17.2	10.8
Total	100.0	100.0

Preparation of Catalysts

A complete block of catalysts has been fabricated using three active metal components impregnated at three levels on a commercial carrier, Katalco extrudates (serial no. 81-6731). Water soluble salts of these metals were selected for the incipient wetness method. Three metal salts chosen are listed below.

1. Ammonium molybdate: $(\text{NH}_4)_6\text{Mo}_7\text{O}_{24} \cdot 4\text{H}_2\text{O}$ (F.W. = 1235.9) with 81.4% assay in MoO_3 (M.W. = 143.94)
2. Cobalt nitrate: $\text{Co}(\text{NO}_3)_2 \cdot 6\text{H}_2\text{O}$ (F.W. = 291.050) with 99.5% purity. The M.W. of CoO is 94.7326.
3. Ammonium Metatungstate: $5(\text{NH}_4)_2\text{O} \cdot 12\text{WO}_3 \cdot 7\text{H}_2\text{O}$ (F.W. = 3168.67) with 99% purity. The M.W. of WO_3 is 231.8482.

The Katalco carrier prior to metal impregnation has the following physical properties [46].

Surface Area: 223 sq m/gm

Pore Volume: 0.933 cu cm/gm

Pore Diameter: 169A

The pore volume distribution data measured by the relative amounts of nitrogen absorbed or desorbed at different absolute pressures is attached in Appendix A.

The sequence of metal loading on a blank carrier has been consistent in the order of Mo, Co, and W throughout the preparation of 27 catalysts. The following procedure served as a general guide for catalyst preparation [47].

1. Drying and calcining the carrier
2. Contacting the carrier with impregnating solution
3. Removing the excess solution
4. Drying and calcination
5. Activation

The carrier was dried at 110°C in an oven and calcined at 500°C in a muffle for 8 hours to obtain the net carrier weight. The volume of the metal solution was determined for each metal impregnation so as to minimize the excess solution of the next metal salt. Generally, the amount of excess solution varied from 30% to 50%. A systematic preparation of 27 catalysts is summarized in Table IV and a 3-D representation is shown in Figure 8. A specific example of calculation for the pore volume is presented in Appendix B.

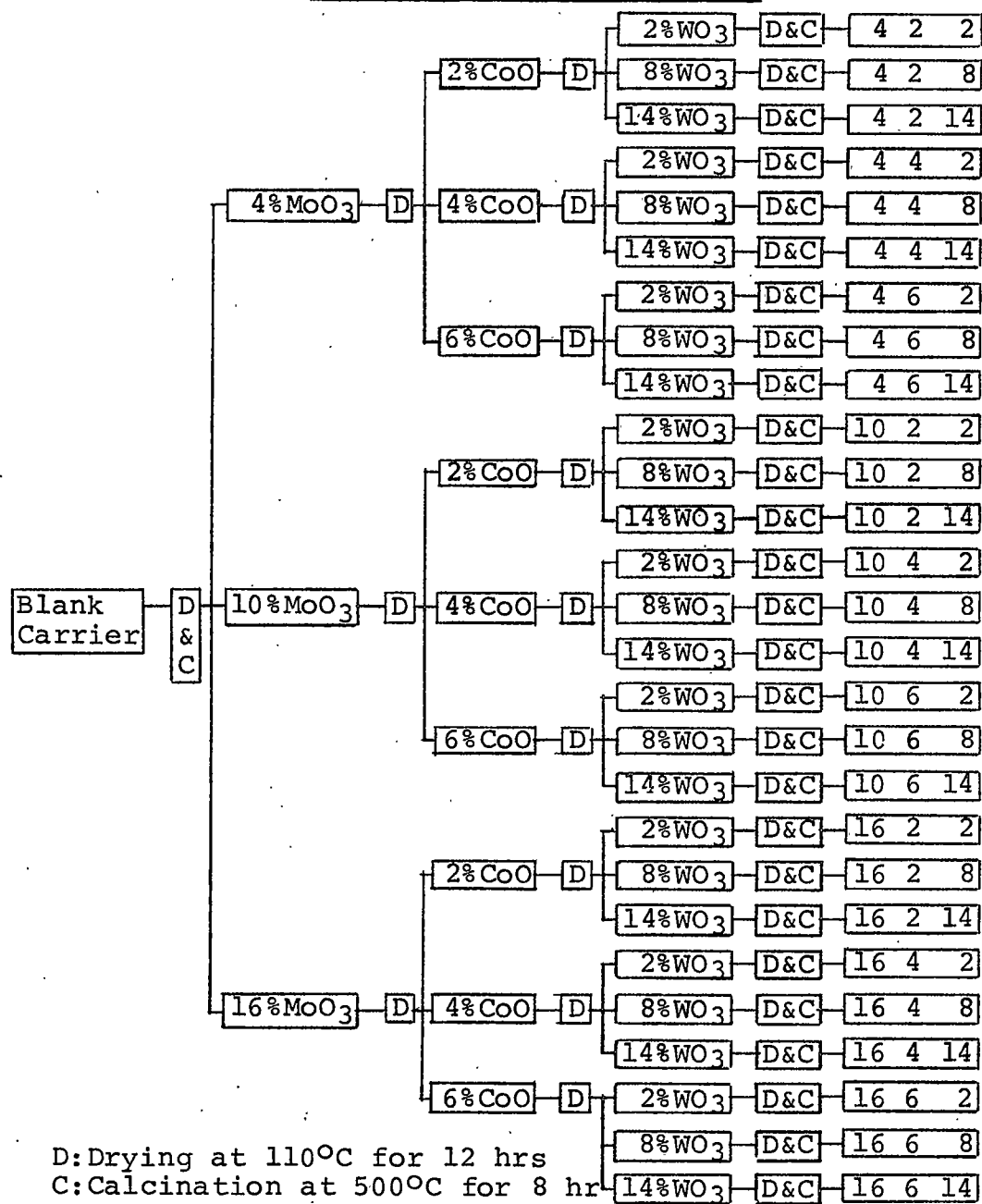
The final metal oxide concentration of a given catalyst by a single impregnation may be calculated from the pore volume and the concentration of solution neglecting selective adsorption [47]. For example, an approximate percent MoO₃ is obtained on the total weight basis as follows, if the pore volume is 1.1 cu cm/gm and MoO₃ concentration in solution is 10.1%.

$$\frac{1.1 \times 0.101}{1 + 1.1 \times 0.101} \times 100 = 10\%$$

The wet catalyst after draining off the excess solution was dried by placing under the draft hood for approximately two hours. Following the oven-drying at 110°C for about

Table IV

Systematic Preparation of 27 Catalysts



D: Drying at 110°C for 12 hrs

C: Calcination at 500°C for 8 hr

Note: %Metal Oxide is defined: (Wt. MO_x/Wt carrier)*100

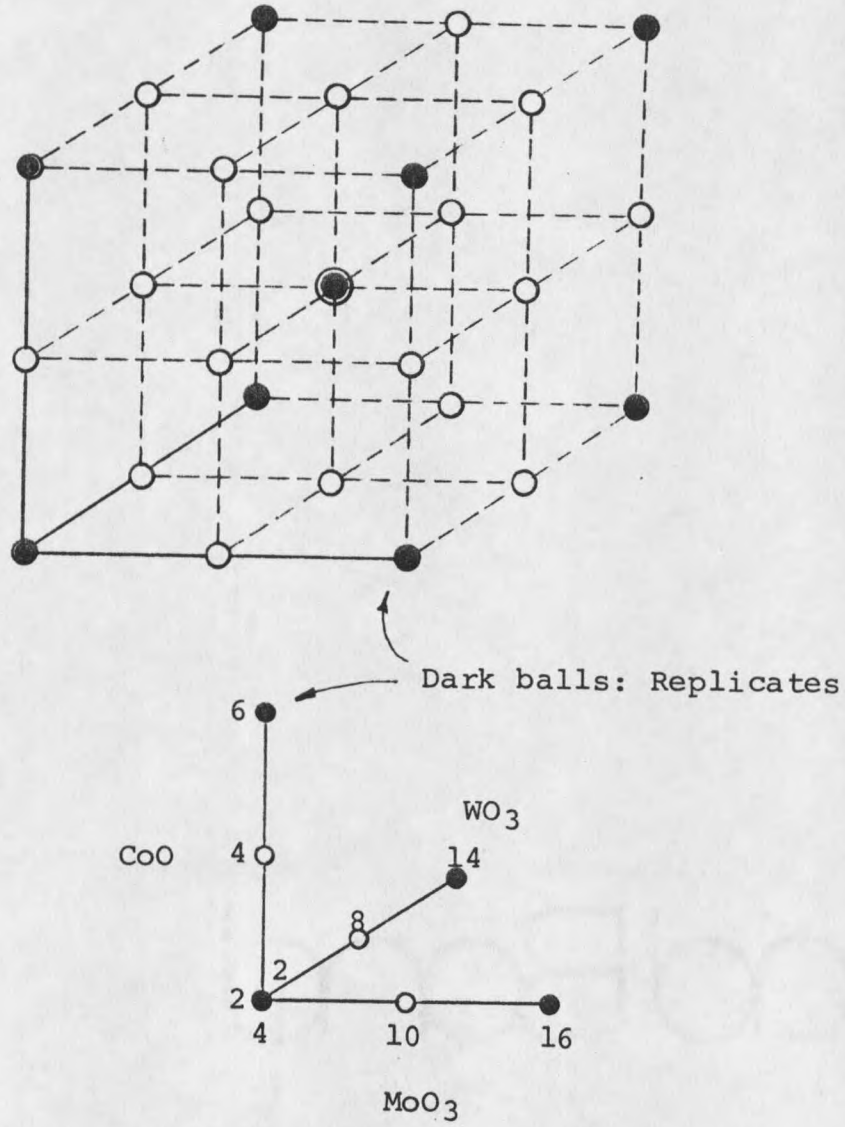


Figure 8. A 3-D representation of 3³ experimental design.

12 hours the catalyst was calcined at 500°C for 8 hours. The calcined catalyst was cooled to room temperature in a desiccator and weighed for final metal concentration.

A batch of catalyst (60 ml) was loaded in a 1 inch diameter sulfiding tube with a concentric thermowell for temperature measurement. The tube was heated to 450°C by an electric furnace while a stream of 10% H₂S in hydrogen passed through the catalyst for 12 hours at 2 to 3 cc per second rate (Figure 9).

The molybdenum, cobalt, and tungsten catalysts were activated by reduction and sulfidation in order to obtain an active catalyst for most reactions in which they are employed (except for oxidation-type reactions). The reduction proceeds gradually and smoothly from the Mo⁺⁶ (W⁺⁶) state to lower valance states (MoS₂ or WS₂) in a stream of 10% H₂S in hydrogen at 450°C [35]. Cobalt oxide is believed to reduce to Co₉S₈ form. Even when presulfiding is not employed, the catalysts become sulfided during processing due to the hydrogen sulfide liberated from the reaction. However, incomplete sulfiding produces catalyst with inferior performance and life.

Sulfided catalysts are known to have better activity than the catalyst in oxidic form. Schuit et al. [48] explained that the bond strength of S-H is significantly lower than that of O-H and a distance between the surface and molybdenum ion is increased by replacement O with S. This may decrease the interaction of π electrons from the N heterorings with molybdenum, resulting in less favorable conditions for surface poisoning by nitrogen bases.

The spent gas from the sulfiding tube was scrubbed by a series of impingers with a 20% NaOH solution. The low concentration (20 to 150 ppm) of H₂S gas can be identified by a distinctive odor similar to rotten eggs.

Exposures of 800 to 1,000 ppm may be fatal in 30 minutes. H₂S does not combine with the hemoglobin of the blood; it's asphyxiant due to paralysis of the respiratory center [49,50].

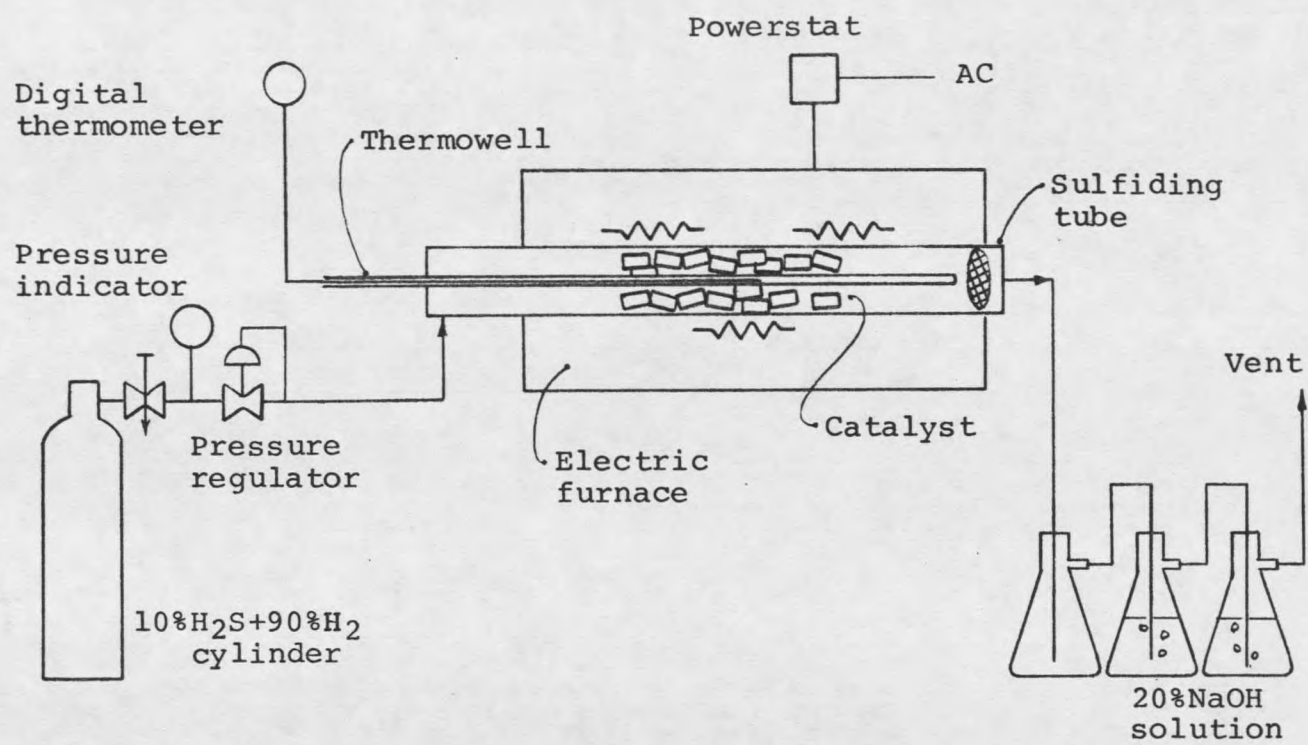


Figure 9. Electric furnace and auxiliary equipment for sulfidation of catalyst.

Continuous Trickle Bed Reactor

The bench scale trickle bed reactor used for this research was fabricated by the Chemical Engineering Department of Montana State University (MSU). A schematic diagram of the trickle bed reactor and its auxiliary equipment is shown in Figure 10.

The reactor consisted of a 1-in. I.D. (35 in. long) schedule-80 Inconel pipe. The top of the reactor was welded with a $\frac{1}{4}$ in. stainless steel cross which allowed the fitting of a 33-in. piece of stainless steel tubing, which served as a thermowell, and the fitting of two feed ports, one for the feed solution and another for hydrogen. The reactor was fitted into the bore of a 6-in. O.D. 3-ft long aluminum block wrapped with three sets of ceramic bead encased NiChrome heating wires. The power to each heating wire was individually controlled by a Powerstat variable autotransformer. A chromel-alumel (type K) thermocouple wire was placed in the $\frac{1}{4}$ -in. stainless steel thermowell at the center of the catalyst section. The temperatures were read by Cole-Palmer digital thermometers (model 8520-40).

To load the catalyst the empty reactor was secured upside down by a vise. The upper space of the reactor was loaded with 175 ml of $\frac{1}{4}$ -in. Norton Denstone, inert ceramic pellets [51], and followed by 25 ml of $\frac{1}{8}$ in. Denstone mainly to preheat and uniformly distribute the feed solution. Sixty ml of catalyst diluted with 60 ml of $\frac{1}{8}$ in. Denstone were loaded [52]. Additional 45 ml of $\frac{1}{8}$ in. Denstone filled the remaining space of the reactor. Finally a stainless steel screen, acting as a support, was placed at the bottom of the reactor before a reactor plug was threaded into the pipe.

The preheated feed solution was metered into the top of the reactor by the use of a Milton Royal simplex piston pump (Model A MR-1-23) through a $\frac{1}{8}$ in. stainless steel tube. The pumping rate was manually controlled by an attached micrometer. All the feed lines and the reservoir were wrapped with flexible heating cords [53] so that the feed temperature was kept around 100°C by the use of Powerstats. Technical grade hydrogen

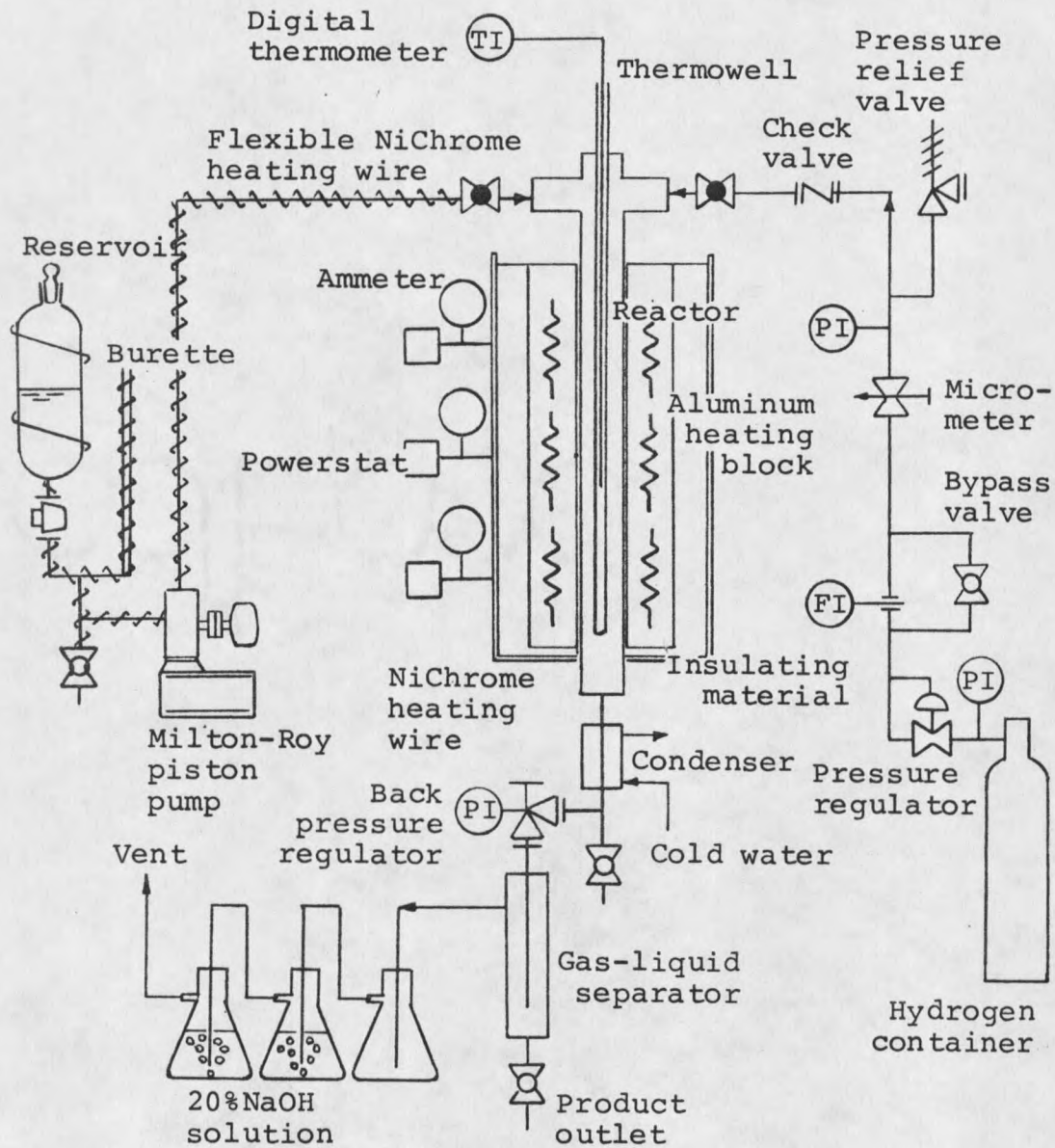


Figure 10. Trickle bed reactor arrangement.

supplied in a cylinder was metered through a pressure regulator by a Brooks thermal mass flowmeter [54].

Hydrogen and feed solution were passed cocurrently through the pressurized reactor (1,000 psig) and then to a gas-liquid separator through a Grove back-pressure regulator equipped with a corrosion-resistant Teflon diaphragm. The exit gases were scrubbed by a 20% NaOH solution and vented. The liquid products were collected in either continuous or periodic mode from the separator.

Operation of Continuous Trickle Bed Reactor

The reactor loaded with the catalyst to be tested was placed in the aluminum heating block. The feed solution and hydrogen lines were connected at the top of the reactor and the separator system was secured at the bottom of the reactor. The thermocouple wire was inserted into the thermowell. All pipe fittings were sealed using either Teflon tape or anti-seize compound (Permatex). The entire system was pressurized to a normal operating range of 1000 psig and checked for leaks using Snoop soap solution. If no leaks were detected, the system was depressurized. Three Powerstats were turned on to heat the reactor to 425°C. When the reactor reached desired reaction temperature, the entire feed system (reservoir, burette, feedlines, check valves, and piston housing) was preheated with NiChrome wires. The hot feed solution was recirculated for a few minutes through the feed line back into the reservoir. Then the feed line was connected to the reactor for operation. The reactor was pressurized with hydrogen through the bypass valve attached to the Brooks flowmeter. When the system approached desired pressure, the bypass valve was closed and the micrometer was adjusted to keep the hydrogen flow to the reactor at a 10,000 scf/bbl rate. The feed solution valve located at the top of the reactor was then opened. The pump was started and the time was logged. The feed rates were measured by timing the liquid level drop in the burette. The feed rate was adjusted by the use of pump

micrometer to a liquid hourly space velocity (LHSV) of 1.0 and frequently checked to ensure a steady flow. The products were collected hourly following the startup, unless otherwise specified.

After the last sample was obtained, the pump was shut off and the liquid feed valve at the top of the reactor was closed. The excessive feed solution was drained from the reservoir and the feed system was cleaned with solvent. The hydrogen valve was shut off and the line was disconnected. The Powerstats were shut off and the separator system was removed after depressurization. The reactor was removed from the aluminum heating block and the entire content of the reactor was dumped in an orderly manner on the collector plate for further inspection. The reactor was cleaned by brushing with acetone.

Analytical Procedure

Hourly liquid products from all runs were analyzed for nitrogen, and a composite sample was analyzed for sulfur to represent the run. The ASTM D-86 distillation was carried out for each composite product. The nitrogen contents were analyzed by the MSU Chemistry Station-Analytical Laboratory using the macro Kjeldahl method [55,56]. Sulfur concentration was determined by the dual unitized quartz tube combustion apparatus [57,58]. Weight percent denitrogenation (% DN) and weight percent desulfurization (% DS) were calculated as follows.

$$\frac{F_{ns} - P_{ns}}{F_{ns}} \times 100 = \% \text{ DN (or \% DS)}$$

where F_{ns} = Wt% nitrogen or wt% sulfur of the feed

P_{ns} = Wt% nitrogen or wt% sulfur of the product.

The extent of hydrocracking was determined by ASTM D-86 distillation. Fifty ml of composite sample representing each catalyst were used as a standard volume. This method measures the cumulative amount of the distilled product which boils below 700°F (370°C) or when decomposition begins [59].

RESULTS AND DISCUSSION

A total of eighty-two batch runs was carried out with a Parr Instrument Company Series 4,000 Pressure Reaction Apparatus for determination of optimum dissolution of SRL in tetralin and for preparation of common feed solution. A complete block of 27 catalysts was tested using a continuous trickle bed reactor. In addition, nine tests of catalysts were duplicated. Finally five special catalysts with different pore diameters were prepared and tested using a large molecular solute as a tracer. The objective of this part of the investigation was to see how meaningful is the average pore diameter of a catalyst, especially when the solute diameter approaches pore diameter.

Preparation of Feed Solution

A mortar and pestle were used to grind chunks of SRL for all runs. The slurry was prepared by mixing powder SRL in tetralin while heating and agitating with a combination magnetic stirrer-heater. Two hundred ml of the resulting slurry (at 130°C) were charged to a 500 ml Parr autoclave. The autoclave cap was then screwed on and the cap bolts were tightened with a torque wrench. The autoclave was pressurized to 1,000 psig with hydrogen and then depressurized to the barometric pressure. This barometric pressure of hydrogen was designated as 0 psig of H₂. The autoclave was again pressurized, if necessary, to a desired final pressure with hydrogen. A summary of the first fourteen autoclave runs is shown in Table V.

The first two runs were made to see if the high temperature could help dissolving the powder SRL in tetralin. The SRL to tetralin ratio of 1:2 was used and the air was not evacuated for these runs. Although the second run (K-2) was extended twice as long in retention time as the first run under the similar operating conditions; both products were

Table V

Summary of the First 15 Batch Runs
(Dissolution of SRL)

Run no.	Gas	Pressure psig	Temperature °C	Retention time hr	SRL Tetralin ratio	Remark
K-1	Air	0	530	1	0.5	Not dissolved
K-2	Air	0	540	2	0.5	Not dissolved.
K-3	H ₂	1000	475	2	0.5	Dissolved
K-4	H ₂	1500	475	2	1	Dissolved. Products
K-5	H ₂	1500	475	2	1	of K-4 through K-7
K-6	H ₂	1500	475	2	1	were used for
K-7	H ₂	1500	475	2	1	Run KC-1.
K-8	H ₂	1500	475	3	1	Dissolved
K-9	H ₂	1500	475	2	1	20 ml of water was
K-10	H ₂	1500	475	2	1	added. Dissolved.
K-11	H ₂	1500	475	1	1	10 ml of water was
K-12	H ₂	1500	475	1	1	added. Dissolved.
K-13	H ₂	1500	475	1	1	5 ml of water was
K-14	H ₂	1500	475	1	1	added. Dissolved
						Products of K-11
						through K-14 were
						used for KC-2

messes of slurries, showing no sign of dissolution. The third run (K-3) was carried out in the same fashion with the pressurized hydrogen instead of air for two hours at 475°C. The product was a liquid with some sediments at room temperature. This progress allowed reducing the SRL to tetralin ratio from 1:2 to 1:1. The following four consecutive runs (K-4 through K-7) were made to prepare feed solution for a continuous trickle bed reactor run.

The catalyst, KN-A, was tested in Run KC-1 using the feed solution decanted from the composite reservoir. In five hours on stream the product became dark and viscous. The operating conditions and the nitrogen and sulfur contents of the hourly products are presented in Table VI. Performance of the catalyst in hydrodenitrogenation is illustrated in Figure 11. The first sign of catalytic deactivation appeared in the fourth hour on stream, and from then on it progressively worsened. The yield was 67.5 wt %.

In an effort to extend the life of the catalyst, a small amount of water was added to the slurry as practiced in the conversion of ethylbenzene to styrene. The Run K-8 was made with a 20 ml of water added to the 200 ml of the slurry under the same reactor conditions as Runs K-4 through K-7. The resulting product showed an excessive water on the top. The amount of water added was gradually reduced to 5 ml for Runs K-10 through K-14. The products from the last four runs were stored and decanted to use as the feed solution for Run KC-2.

The same catalyst, KN-A, was tested again using the water added feed solution for 7 hours (Run KC-2). The nitrogen and sulfur contents of the hourly products are summarized in Table VI. The effect of addition of water to the pretreated feed solution on the catalytic activity is illustrated in terms of denitrogenation and desulfurization (Figure 11). It appears that the effect of 2.5 wt % water present in the feed was insignificant. In fact, a slight degradation in catalytic activity with the water could partially be attributed to the lower feed reservoir temperature. A normal reservoir temperature of 100°C had to be

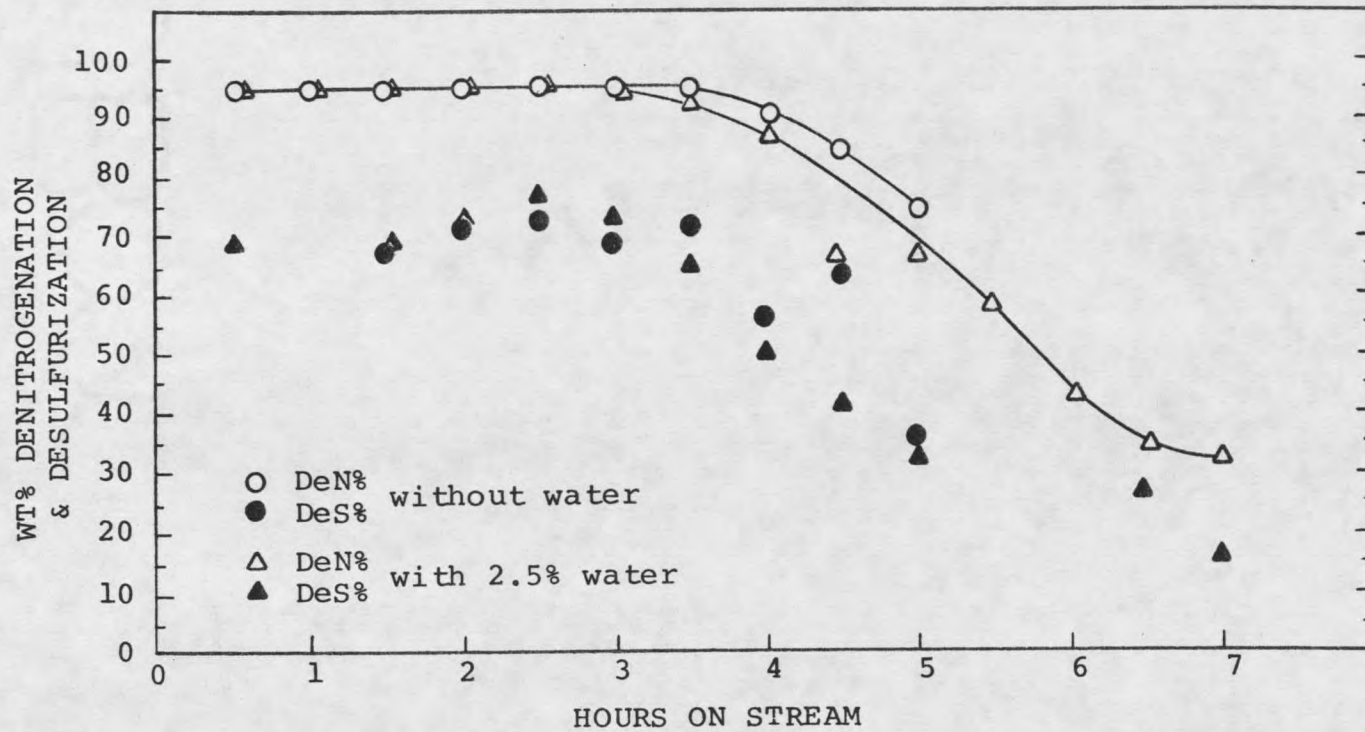


Figure 11. Effect of water addition in wt% denitrogenation and wt% desulfurization.

lowered to 80°C to prevent the boiling of excessive water still present. Lipsch and Schuit (1969) observed strong adsorption of water on the surface of molybdenum-cobalt catalyst supported on alumina, resulting in poisoning of HDS of thiophene and hydrogenation of butenes [60]. This suggests that water might be adsorbed on active sites, leaving less available to the reactions. However, an increase in yield was experienced when water was added.

Two previous sets of autoclave operating conditions were arbitrarily adopted to provide the feed solutions for Run KC-1 and the water-added feed solution for Run KC-2. The autoclave operating conditions were reevaluated by a factorial experiment. Runs K-15 through K-27 were made for this purpose. The SRL dissolubility in tetralin was gauged by the weight percent sediment of centrifugation. The pretreated feed solution was cooled to the room temperature and centrifuged at 2,200 rpm for 5 minutes to determine the weight percent sediment. Zero percent sediment means a complete dissolution. Any value less than 10% was considered as "good." Three factors in this experiment were considered as rows, groups and columns, each at two, two, and three levels respectively. This gave 12 possible combinations. The results are summarized in Table VII and presented in Figure 12. As can be seen from the figure, the effect of retention time on the dissolubility is most significant.

The ranges of the three key variables (temperature, hydrogen pressure, and retention time) were further extended for the final optimization. The results of thirteen autoclave runs are summarized in Table VIII. Run K-28 was made to see if the extended retention time (4 hours) would enhance the dissolution. Contrary to the expectation, a hard solid deposit was observed on the wall, resulting in a record high of 62.3% sediment. The same operating conditions were used for Run K-29 except a retention time of 0 hour. The result was good with 6.9% sediment without any visible carbonaceous deposit.

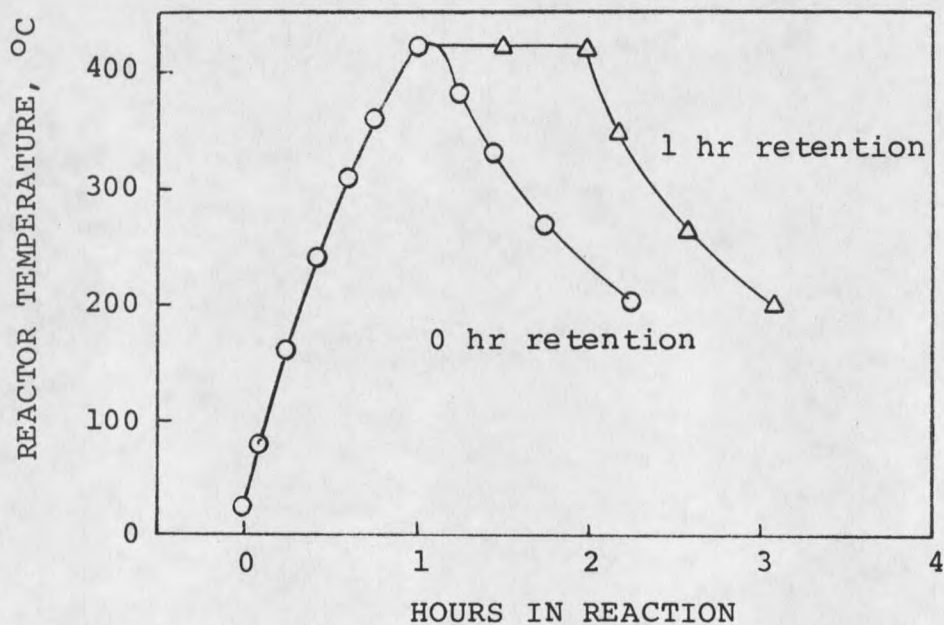
The reaction temperature was reduced to 525°C from 575°C in Run K-30. The weight percent sediment was increased to 17.7% for zero hour retention time. This value

Table VII

SRL Dissolubility at Various Operating Conditions

Retention time, hr	Pressure, psig	Wt% sediment			
		375°C	425°C	475°C	525°C
0*	0	56.3 (K-15)	40.6 (K-16)	37.5 (K-17)	44.7 (K-23)
0	1000	46.3 (K-18)	41.9 (K-19)	38.6 (K-20)	
1	0	51.4 (K-21)	32.0 (K-22)	18.7 (K-24)	
1	1000	60.3 (K-25)	34.9 (K-26)	15.5 (K-27)	

* A retention time of 0 hr means that the autoclave was brought to the desired temperature and then the heater was turned off immediately. See below.



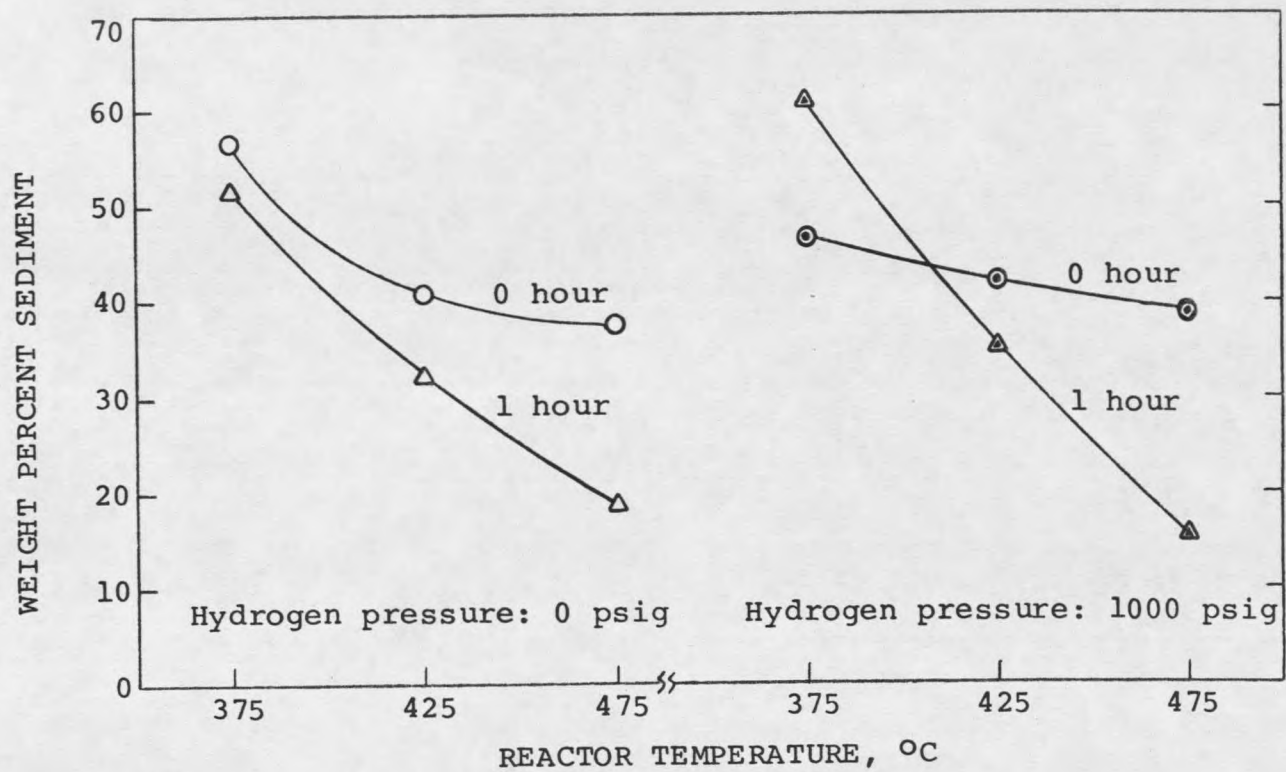


Figure 12. Effect of reactor temperature and retention time at two levels of hydrogen pressure on SRL dissolubility in tetralin.

Table VIII

SRL Dissolubility at Extended Operating Conditions

Retention time hr	Hydrogen pressure psig	Wt% sediment			
		425°C	475°C	525°C	575°C
0	1000	-	-	17.7 (K-30)	6.9 (K-29)
0	2000	-	43.6 (K-36)	-	-
1/6	2000	-	35.0 (K-37)	-	-
1/3	2000	-	27.3 (K-39)	-	-
1/3	3000	-	6.7 (K-40)	-	-
1/2	2000	-	6.9 (K-38)	-	-
1	1000	-	-	3.5 (K-31)	-
1	2000	46.4 (K-33)	4.7 (K-35)	-	-
2	1000	-	5.9 (K-32)	-	-
4	1000	-	-	-	62.3 (K-28)
4	2000	12.6 (K-34)	-	-	-

was reduced to a record low of 3.5% when the retention time was increased to 1 hour as experienced with Run K-31. However, due to frequent problems with the electrical heating unit the maximum allowable temperature had to be limited to 475°C. Therefore, the remainder of the batch runs were carried out to optimize the other two variables, hydrogen pressure and retention time. The weight percent sediments obtained from three runs (K-29, K-30, and K-31) were added and the results of the extended experiments are shown in Figure 13. The dissolution improved as the reaction temperature increased. The two curves, zero hour retention vs. one hour retention, ran in parallel at a weight percent sediment of less than 37%. This trend indicates that the reduced reaction temperature could be compensated to some extent by longer retention time.

Next, attention was focused on the role of the initial hydrogen pressure in dissolution. Figure 14 showed two contrasting curves. The lower curve was constructed based on the data obtained under the various initial hydrogen pressures at a fixed retention time (1 hour) and at a constant reaction temperature (475°C). The upper curve was plotted with the data obtained under the same operating conditions except a constant reaction temperature of 425°C. It appeared that the higher initial hydrogen pressure enhanced the dissolution of SRL in tetralin only at a certain reaction temperature (475°C) or higher (Figure 14).

Finally, efforts were made to determine the optimum retention time with the other two fixed variables (475°C and 2,000 psig H₂). Figure 15 indicated that there was a drastic improvement in dissolution when the retention time had been increased from 20 minutes to 30 minutes. It appeared that a retention time of at least 30 minutes should be allowed if the reaction temperature of 475°C and the initial hydrogen pressure of 2,000 psig were chosen. It was also found that the initial hydrogen pressure of 3,000 psig could reduce the retention time from 30 minutes to 20 minutes. However, the initial hydrogen pressure of 2,000 psig was more practical with the existing equipment at hand. The optimized operating conditions for the maximum dissolution are:

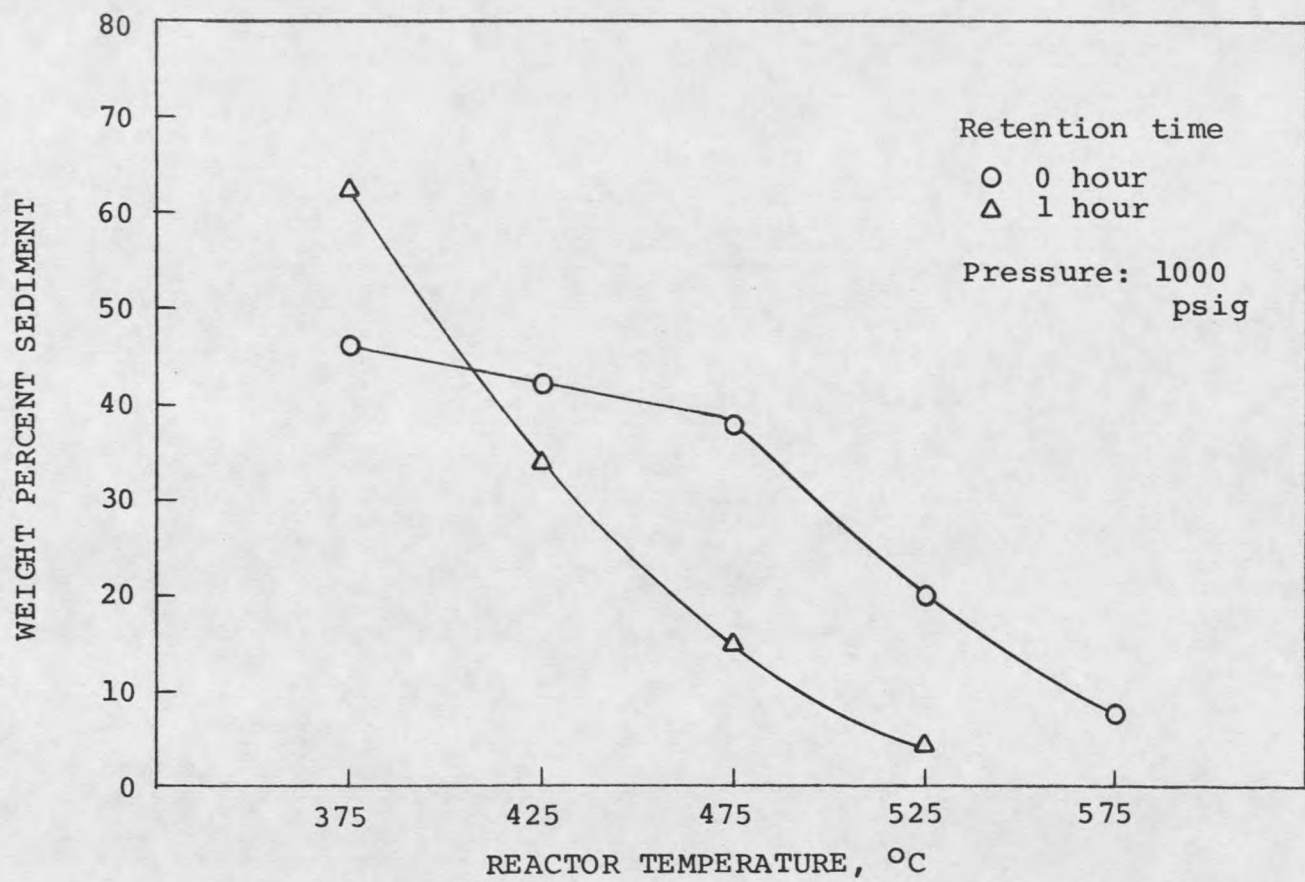


Figure 13. Effect of reactor temperature on SRL dissolubility in tetralin at two levels of retention time.

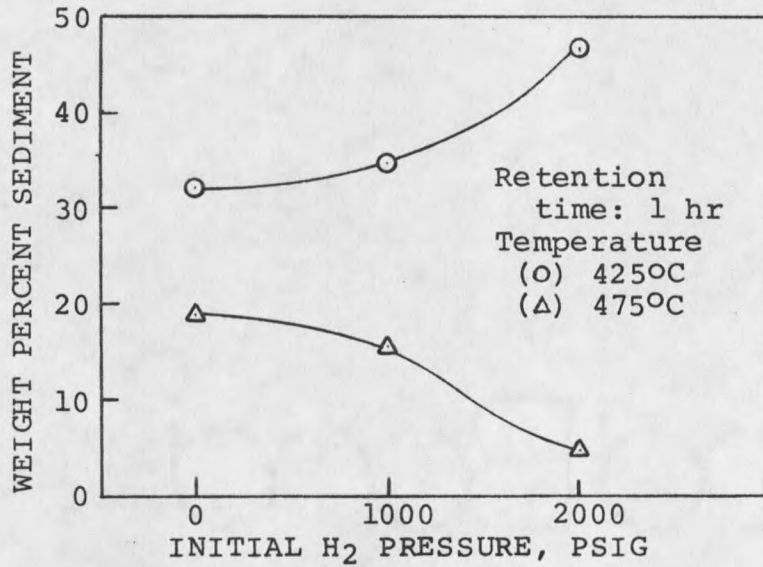


Figure 14. Effect of hydrogen pressure on SRL dissolubility at two different temperature levels.

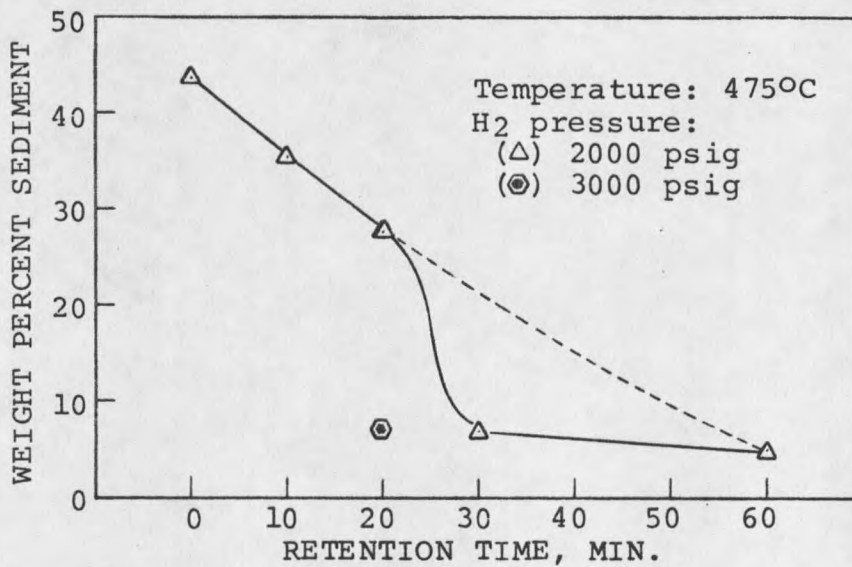


Figure 15. Effect of retention time on SRL dissolubility in tetralin at 475°C and 2000 psig of H₂.

1. Reactor temperature = 475°C
2. Initial hydrogen pressure = 2,000 psig
3. Retention time = 40 minutes

The batch runs from K-40 through K-82 were made with these optimum operating conditions for the common feed solution. The feedstock thus prepared was used to evaluate the 27 catalysts in the continuous trickle bed reactor.

Performance Tests

A total of thirty-seven runs have been completed with a continuous trickle bed reactor; a randomized complete design of twenty-seven catalysts, fractional replications of 9 catalysts, and a blank carrier. The first two runs were carried out for 8 hours; the first with blank carrier and the second with K-14 catalyst. The nitrogen contents of hourly product samples are presented in Table IX. Performance of the KT-14 catalyst is illustrated in Figure 16 in comparison with that of a blank carrier. Although the K-14 catalyst is superior in denitrogenation to the blank carrier, there is a striking similarity between these two curves. The abrupt changes in denitrogenation during the second and third hour on stream were partially attributed to the gradual plugup of pores by the suspended solid particles in the feed and partially to the wide pore distribution of the catalysts. The latter is explained further in "Development of A Model for Catalyst." The remainder of catalysts were tested for four hours and the product samples were taken hourly for analysis. The reactor operating conditions are kept constant at $425 \pm 5^\circ\text{C}$, 1,000 psig, LHSV of 1.0 and hydrogen flow rate of 10,000 scf per barrel of feed.

The nitrogen contents of hourly products are shown in Table X. The average weight percent nitrogen concentration was calculated based on the hourly nitrogen values and the amount of the hourly product. The average denitrogenation (Table X) was based on

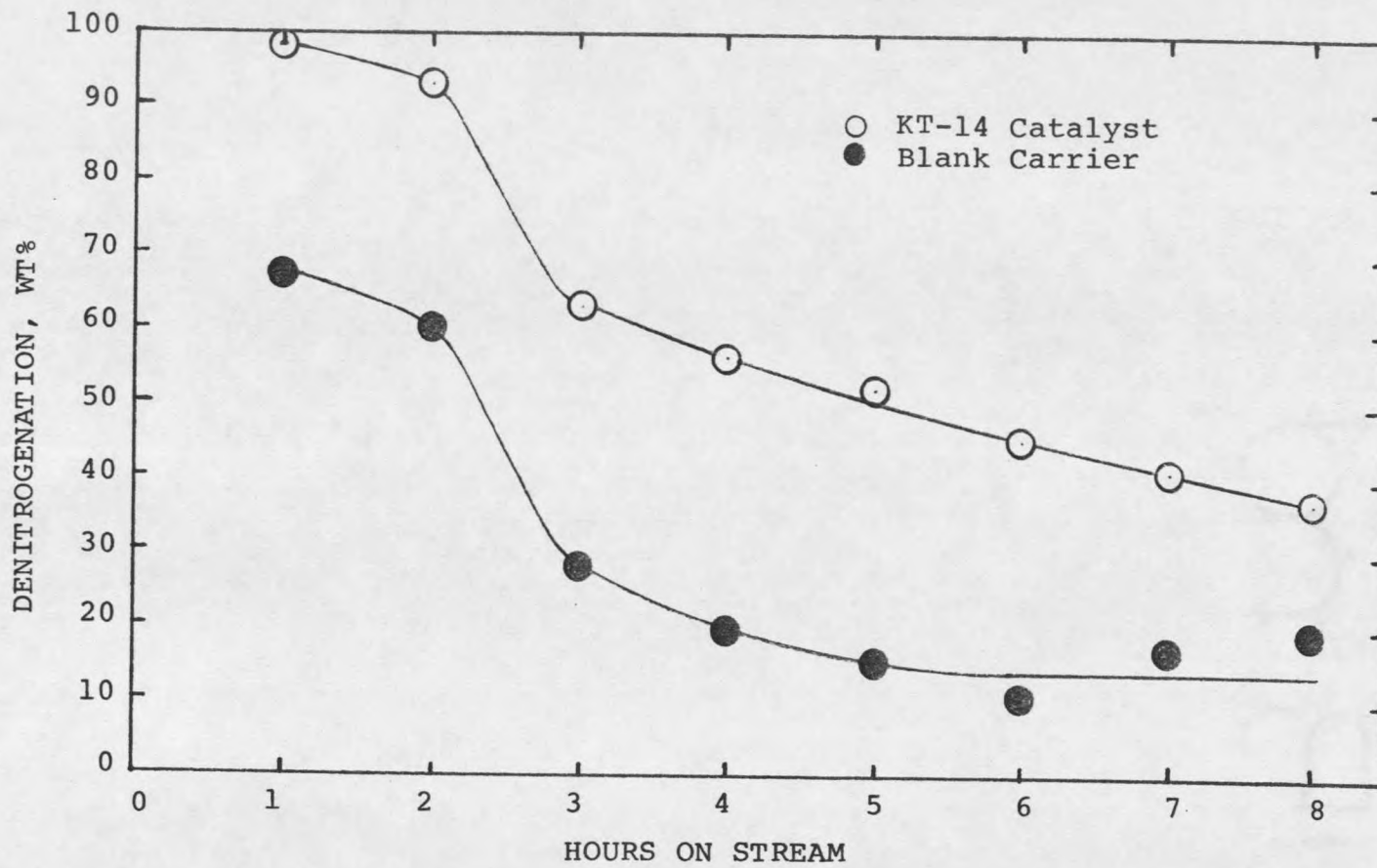


Figure 16. Catalytic performance of KT-14 against blank base in denitrogenation.

Table X

Nitrogen Removal With KT Series Catalysts

Cat. No.	Nitrogen concentration, wt%				Avg	DeN%
	Hours on stream					
	1	2	3	4		
Blank	0.15	0.18	0.33	0.37	0.276	40.0
KT-1	0.05	0.11	0.24	0.25	0.184	59.9
KT-2	0.01	0.04	0.20	0.23	0.146	68.3
KT-3	0.03	0.08	0.24	0.27	0.179	61.1
KT-4	0.01	0.03	0.17	0.22	0.135	70.7
KT-5	0.01	0.03	0.16	0.23	0.135	70.7
KT-6	0.01	0.03	0.16	0.23	0.137	70.2
KT-7	0.01	0.07	0.18	0.25	0.168	63.4
KT-8	0.01	0.04	0.16	0.23	0.131	71.5
KT-9	0.02	0.05	0.20	0.21	0.144	68.8
KT-10	0.02	0.04	0.19	0.24	0.149	67.6
KT-11	0.01	0.04	0.17	0.24	0.143	68.9
KT-12	0.02	0.05	0.24	0.25	0.166	64.0
KT-13	0.01	0.05	0.14	0.19	0.113	75.4
KT-14	0.01	0.03	0.17	0.20	0.125	72.8
KT-15	0.02	0.05	0.14	0.23	0.140	69.6
KT-16	0.01	0.03	0.16	0.25	0.136	70.4
KT-17	0.01	0.03	0.16	0.22	0.132	71.3
KT-18	0.02	0.05	0.20	0.20	0.137	70.2
KT-19	0.01	0.05	0.19	0.25	0.158	65.6
KT-20	0.01	0.07	0.20	0.24	0.157	65.9
KT-21	0.01	0.06	0.21	0.24	0.169	63.2
KT-22	0.04	0.05	0.18	0.24	0.120	73.8
KT-23	0.02	0.08	0.19	0.22	0.148	67.9
KT-24	0.01	0.03	0.22	0.26	0.163	64.6
KT-25	0.01	0.04	0.16	0.23	0.138	70.0
KT-26	0.02	0.05	0.19	0.28	0.157	65.8
KT-27	0.01	0.05	0.23	0.25	0.170	63.0
KT-1R	0.04	0.10	0.24	0.25	0.182	60.5
KT-3R	0.03	0.07	0.25	0.28	0.183	60.3
KT-7R	0.02	0.07	0.23	0.26	0.176	61.5
KT-9R	0.03	0.06	0.20	0.22	0.149	67.5
KT-14R	0.01	0.03	0.16	0.20	0.122	73.5
KT-19R	0.02	0.06	0.21	0.26	0.162	64.7
KT-21R	0.01	0.06	0.22	0.26	0.166	64.0
KT-25R	0.02	0.05	0.18	0.23	0.144	68.4
KT-27R	0.02	0.05	0.23	0.28	0.176	61.7

the average weight percent nitrogen content of the products and the initial nitrogen content of the feed (0.46%).

The result of the ASTM D-86 distillation for all the composite products representing each catalyst and blank carrier are presented in Appendix C. From these data, typical ASTM distillation curves were constructed to illustrate the stepwise transformations of SRL to distillate fuel. Figure 17 shows the two starting materials (SRL + tetralin), pretreated feed solution, and the catalytically hydrocracked product with the KT-17. The blank carrier showed some influence on hydrocracking of the SRL. The best results were obtained with the K-17 catalyst (10% MoO₃, 6% CoO, and 8% WO₃). The hydrocracking parameter was obtained from the ASTM distillation curve. Due to difficulties in dealing with the curves, two criteria (hydrocracking parameters) have been introduced: (1) the percentage of gasoline distilled up to 380°F (193°C) and (2) the percentage of residue remaining in the pot at 450°F (232°C). These two values were used to characterize the distillation products. The lower the percentage of residue with a larger portion of gasoline, the better.

The average desulfurization obtained from the sulfur content of composite products and the feed is also presented in Table XI along with the hydrocracking parameter (% distillate) and product yield.

Effect of Metal Compositions on Upgrading

The effect of three active metals impregnated on Katalco carrier on upgrading of SRL were evaluated in three major categories: denitrogenation, desulfurization, and hydrocracking. Each of these dependent variables was correlated with three independent variables (factors): MoO₃, CoO and WO₃. A statistical analysis was performed with the aid of a computer to obtain multiple linear regressions using data transformations [61].

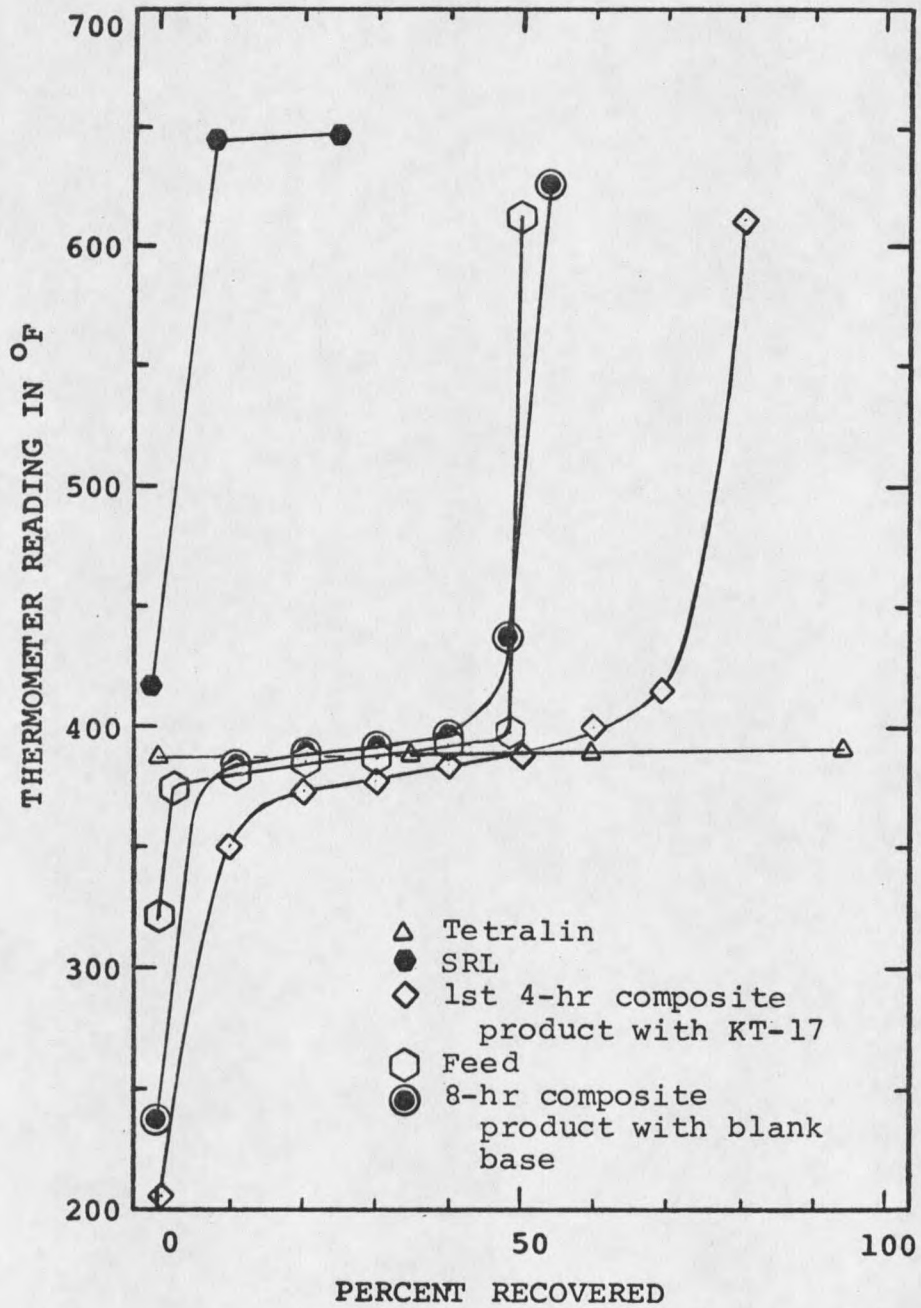


Figure 17. ASTM D-86 distillation, feed and 8-hr composite product of blank carrier.

Table XI
Summary of Catalytic Performance

Cat. No.	DeN%	DeS%	% Distillate		Yield
			380°F	450°F	
Blank	40.0	4.5	9	57	53.3
KT-1	59.9	52.5	17	63	72.3
KT-2	68.3	57.5	20	69	70.2
KT-3	61.1	55.3	29	71	79.4
KT-4	70.7	69.0	13	62	72.1
KT-5	70.7	72.1	24	65	72.3
KT-6	70.2	70.6	26	70	70.4
KT-7	63.4	61.5	15	62	79.8
KT-8	71.5	70.5	23	62	70.2
KT-9	68.8	69.0	30	72	72.9
KT-10	67.6	68.7	30	71	74.8
KT-11	68.9	67.4	25	62	73.5
KT-12	64.0	65.6	29	71	73.8
KT-13	75.4	76.5	26	72	72.7
KT-14	72.8	77.7	20	62	71.7
KT-15	69.6	72.7	25	62	74.2
KT-16	70.4	66.9	30	72	71.7
KT-17	71.3	72.5	34	72	72.9
KT-18	70.2	70.5	30	72	75.6
KT-19	65.6	58.5	30	72	74.2
KT-20	65.9	56.5	10	65	74.2
KT-21	63.2	54.6	20	70	67.3
KT-22	73.8	70.0	10	68	74.8
KT-23	67.9	65.1	13	67	76.3
KT-24	64.6	67.5	10	67	73.8
KT-25	70.0	63.9	17	67	73.8
KT-26	65.8	68.0	13	68	76.3
KT-27	63.0	50.0	10	68	74.2
KT-1R	60.5	54.2	16	64	78.8
KT-3R	60.2	53.6	28	70	75.8
KT-7R	61.5	56.8	17	62	75.8
KT-9R	67.5	68.5	28	72	77.9
KT-14R	73.5	77.2	21	63	75.6
KT-19R	64.7	51.8	30	72	75.8
KT-21R	64.0	56.3	19	70	79.0
KT-25R	68.4	65.7	18	67	73.8
KT-27R	61.7	53.7	12	70	75.8

Figure 18 was plotted to show the weight percent denitrogenation as a function of weight percent MoO_3 , neglecting the presence of the other two metals. The role of these active metals in denitrogenation was clearly seen as compared to the blank carrier, and the quadratic effect of MoO_3 concentration was significant. Further breakdown to three levels of CoO and WO_3 concentrations is illustrated in Figure 19. Each curve shows a quadratic trend with a local maximum denitrogenation at around 10% MoO_3 concentration and there are some interactions. Further increase in MoO_3 content failed to demonstrate any benefit. The global maximum denitrogenation was attained approximately at 10% MoO_3 , 4% CoO and 6% WO_3 . The nitrogen removal as an explicit function of CoO is shown in Figure 20 and the details of individual correlation is shown in Figure 21. These two figures also confirmed that the maximum nitrogen removal was achieved at around 4% CoO concentration. The effect of tungsten concentration on denitrogenation is explicitly illustrated in Figure 22. Unlike the two previous curves the presence of 2% WO_3 appeared to be as effective as any higher concentrations. Figure 23 shows this trend in detail. At low MoO_3 level (4%), an increase in WO_3 up to 8% generally improved the denitrogenation. However, at higher MoO_3 levels (10% and 16%) any addition of WO_3 beyond 2% level actually impaired catalytic performance in denitrogenation.

An analysis of variance (ANOVA) for three factors at three levels is shown in Table XII. An unweighted means procedure was used for unequal replications. The ANOVA table is a statistical technique used to determine those factors having a significant effect on denitrogenation. The first F value of the fifth column greater than 4.26 designates the factor that is significant at a significance level of 5%. That is, if the parameter is determined to be significant, there is only one chance in twenty of being in error. Since the F-values are greater than 4.26, each parameter has a significant effect.

Table XIII shows multiple linear regression which was obtained by the use of backward stepwise regression technique at a significant level of 5%. Thus, regression equation

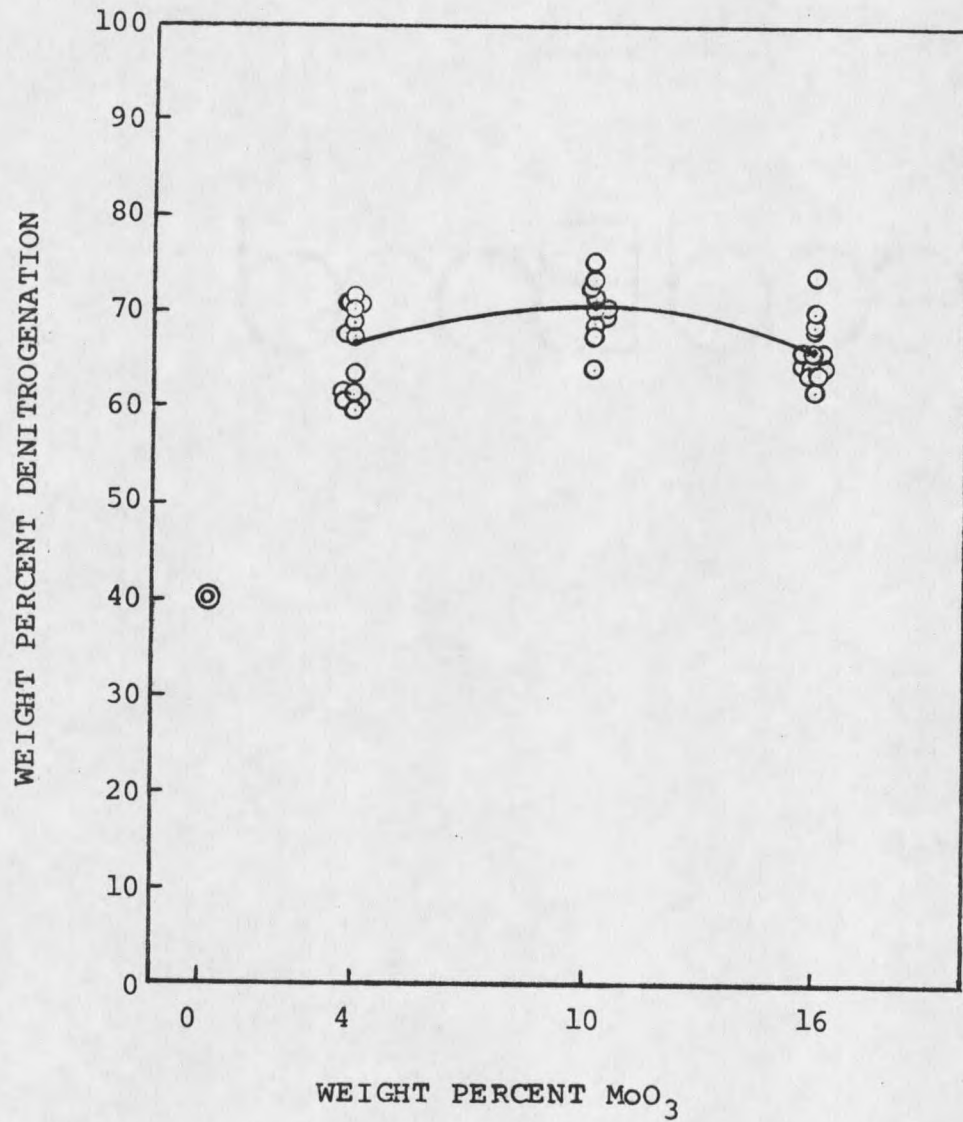


Figure 18. Catalytic performance in denitrogenation as a function of MoO₃ concentration.

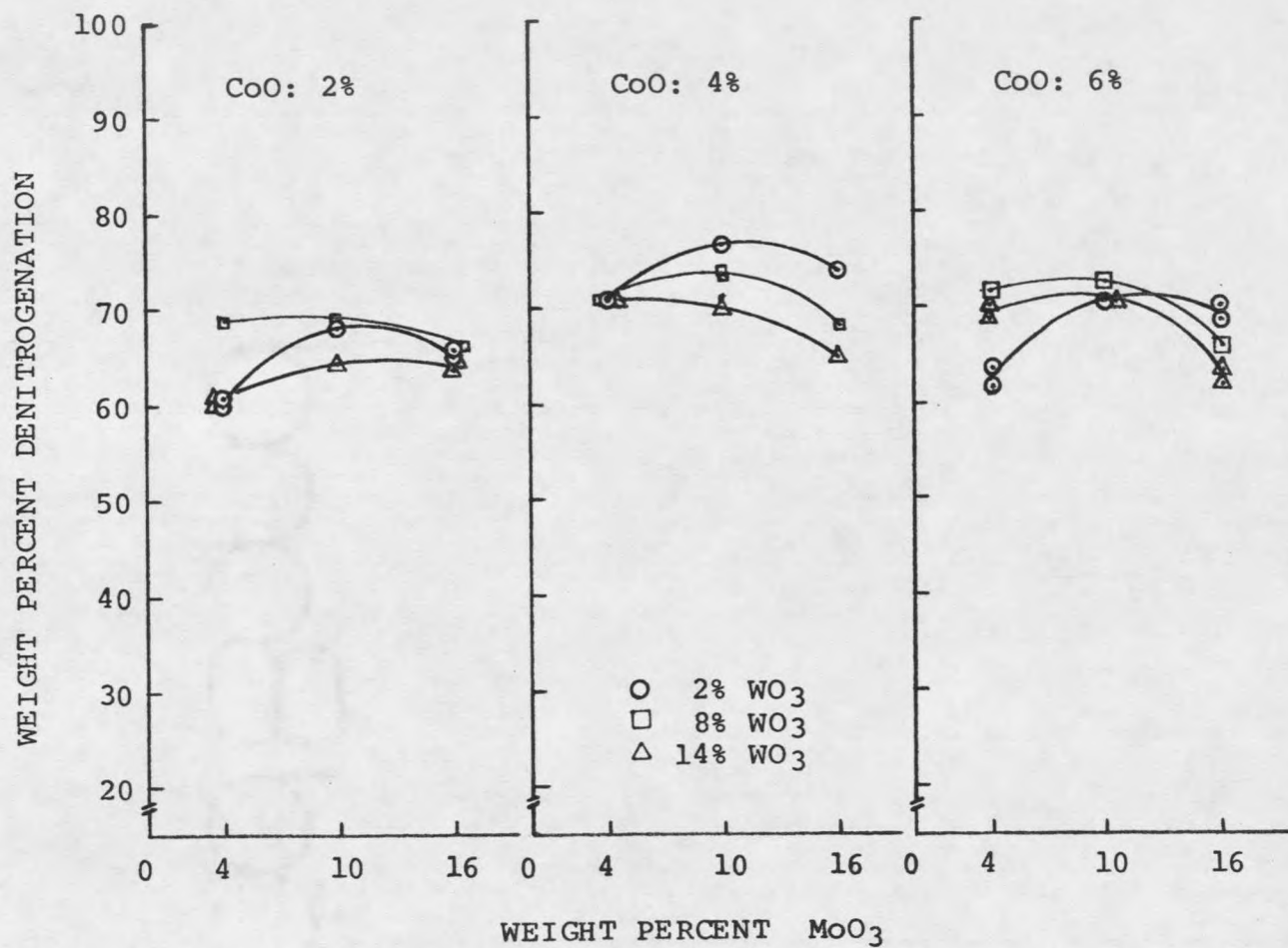


Figure 19. Catalytic performance in denitrogenation as a function of CoO, WO₃, and MoO₃ concentrations.

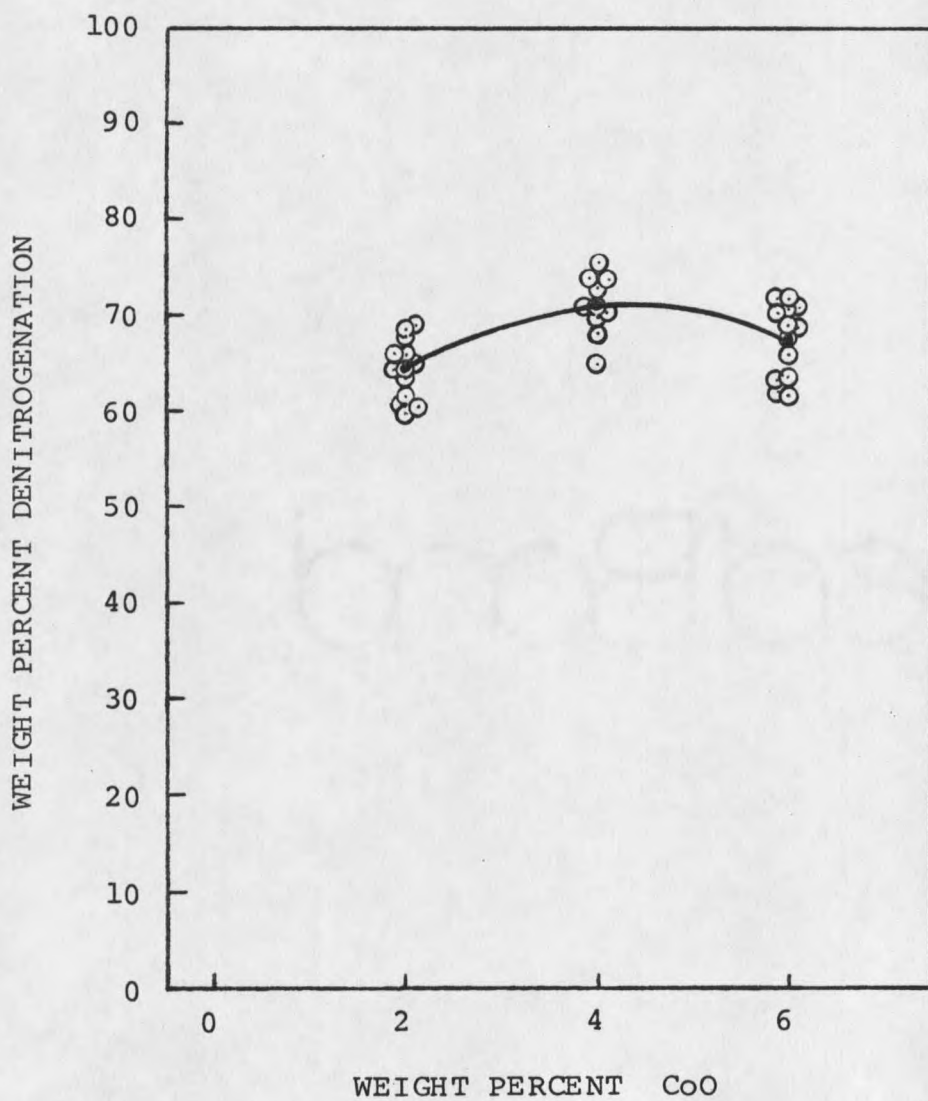


Figure 20. Catalytic performance in denitrogenation as a function of CoO concentration.

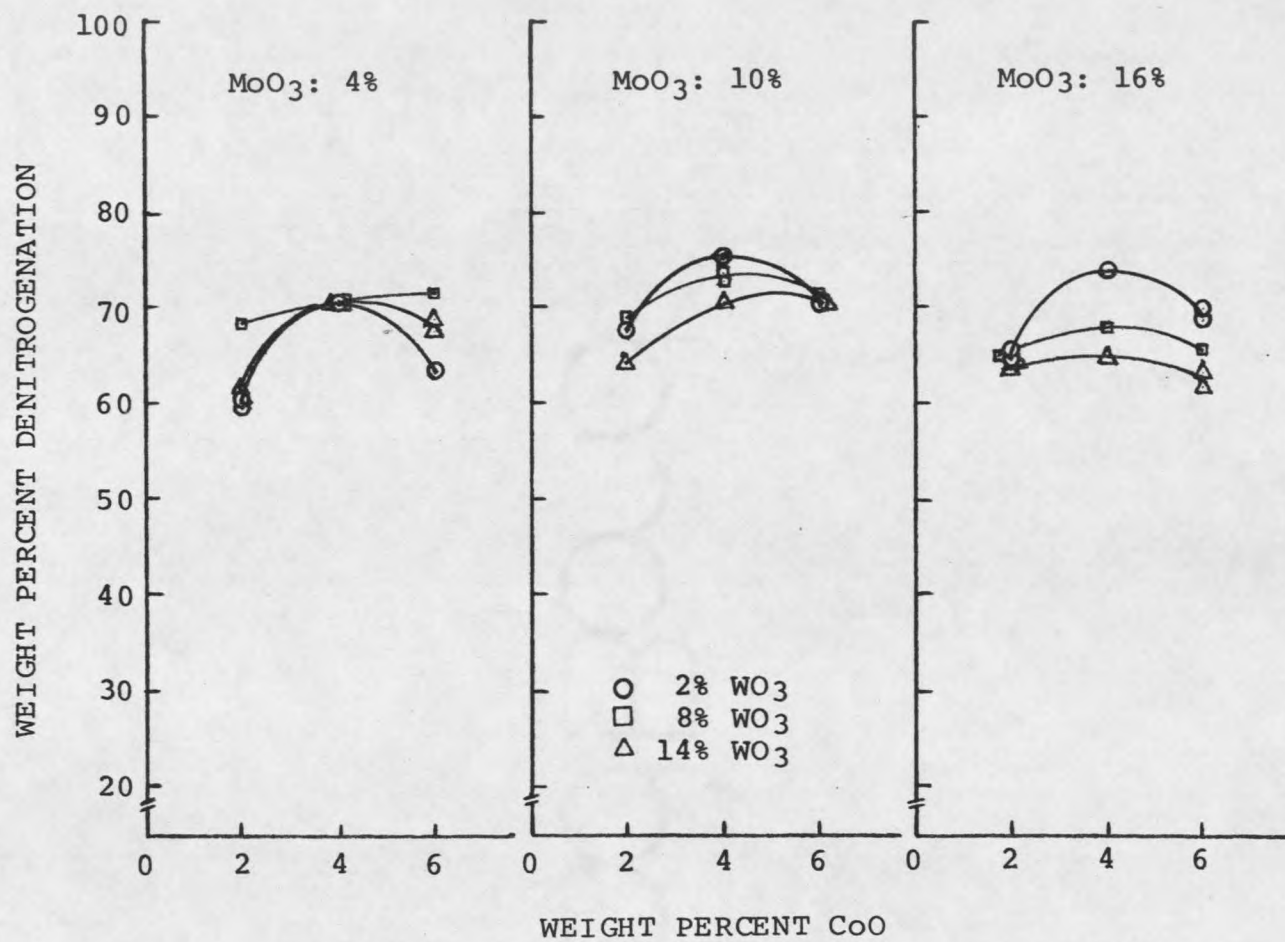


Figure 21. Catalytic performance in denitrogenation as a function of MoO₃, WO₃, and CoO concentrations.

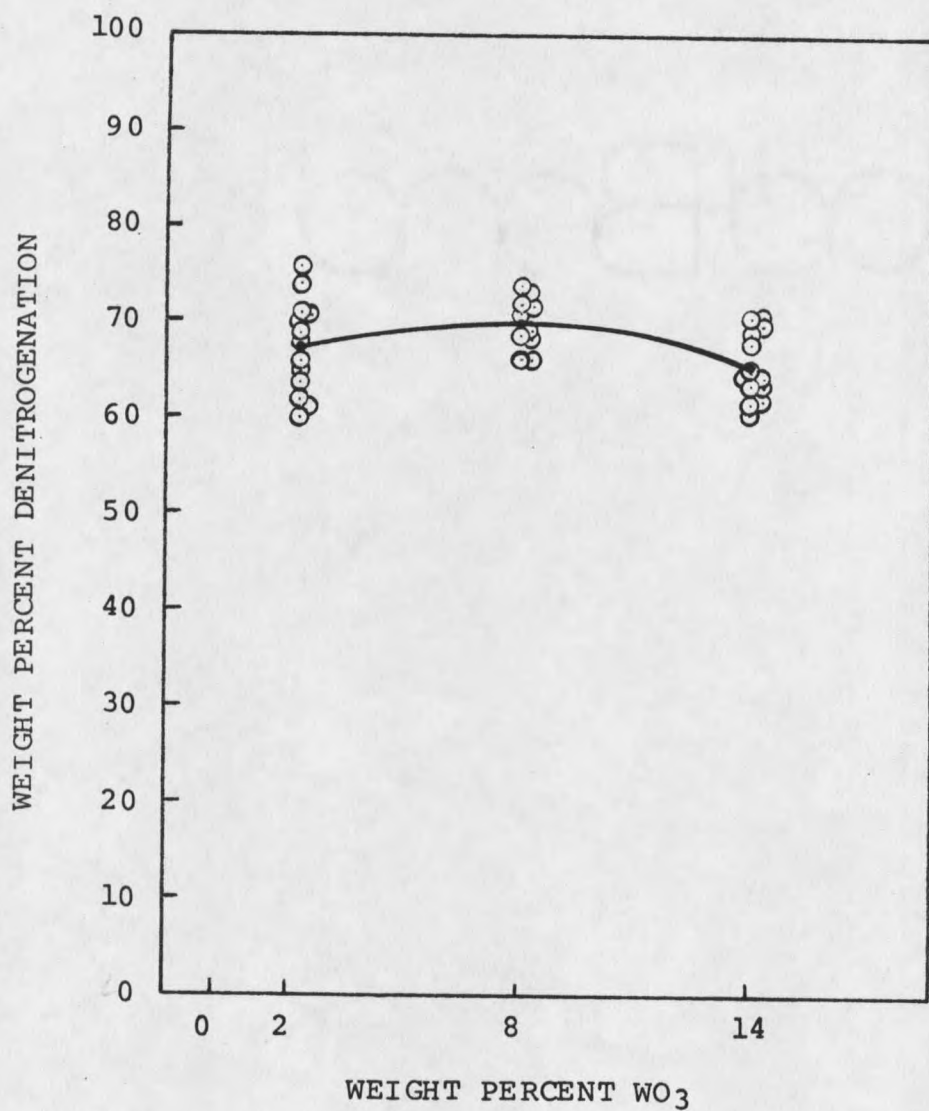


Figure 22. Catalytic performance in denitrogenation as a function of WO_3 concentration.

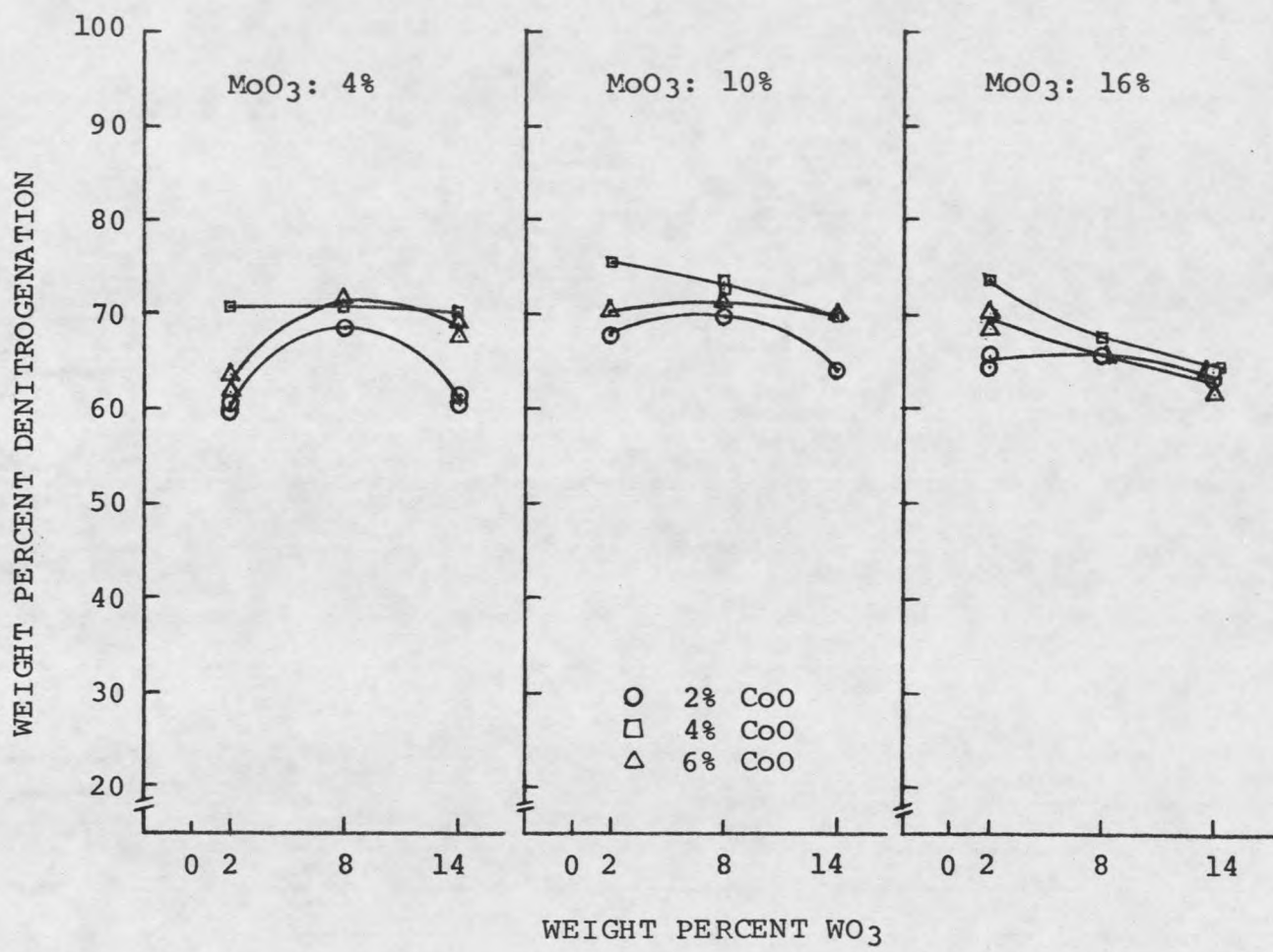


Figure 23. Catalytic performance in denitrogenation as a function of MoO₃, CoO, and WO₃ concentrations.

Table XII

Analysis of Variance for Three Factors at Three Levels

CELL COUNTS ARE UNEQUAL. ANALYSIS IS BASED ON UNWEIGHTED MEANS.
UNWEIGHTED MEANS & COUNT OF CELL MEANS PER MEAN FOLLOW:

FACTOR = 1
 TRT N MEANS
 4 9 66.98
 10 9 70.06
 16 9 66.48

FACTOR = 2
 TRT N MEANS
 2 9 64.92
 4 9 70.67
 6 9 67.93

FACTOR = 3
 TRT N MEANS
 2 9 68.32
 8 9 69.27
 14 9 65.93
 HARMONIC CT= 1.200

ANALYSIS OF VARIANCE:

SOURCE	DF	S.S.	M.S.	F-VALUE	P-VALUE
1	2	67.71	33.85	57.76	0.000
2	2	148.9	74.44	127.0	0.000
1 2	4	13.96	3.491	5.955	.1292E-01
1 3	2	53.46	26.73	45.61	0.000
1 3	4	69.47	17.37	29.63	0.000
2 3	4	36.92	9.230	15.75	.7309E-03
1 2 3	8	23.96	2.995	5.110	.1295E-01
RESIDUAL	9	5.275	.5861		

Three Levels

Factor 1 = Wt% MoO ₃	4%	10%	16%
Factor 2 = Wt% CoO	2%	4%	6%
Factor 3 = Wt% WO ₃	2%	8%	14%

Response Variable = Wt% denitrogenation

Table XIII

Multiple Regression Analysis for Denitrogenation

DEPENDENT VARIABLE = 4

INDEPENDENT VARIABLES= 1 2 3 12 13 14 17

FIT:	VAR	R-PART	B	SE(B)	T	P-VALUE
	1	.6615	2.330	.4991	4.667	0.000
	2	.7124	9.370	1.744	5.372	0.000
	3	.5233	1.352	.4161	3.250	.3002E-02
	12	-.5949	-.9410E-01	.2403E-01	-3.916	0.000
	13	-.6851	-1.076	.2163	-4.976	0.000
	14	-.4339	-.6123E-01	.2403E-01	-2.548	.1659E-01
	17	-.5760	-.5250E-01	.1408E-01	-3.728	0.000

INTERCEPT = 37.43

R-SQUARED = .7705

ANALYSIS OF VARIANCE:

SOURCE	DF	S.S.	M.S.	F-VALUE	P-VALUE
REGRESS	7	483.1	69.02	13.43	0.000
RESIDUAL	28	143.9	5.140		
TOTAL	35	627.1			

- 4 = Wt% denitrogenation
 1 = Wt% MoO₃
 2 = Wt% CoO
 3 = Wt% WO₃
 12 = (Wt% MoO₃) (Wt% MoO₃)
 13 = (Wt% CoO) (Wt% CoO)
 14 = (Wt% WO₃) (Wt% WO₃)
 17 = (Wt% MoO₃) (Wt% WO₃)

(the weight percent denitrogenation regressed on the metal oxide concentrations) is constructed as follows.

$$\begin{aligned} \text{Wt\% DeN} = & 37.43 + 2.33 (\text{MoO}_3) + 9.37 (\text{CoO}) + 1.35 (\text{WO}_3) \\ & - 0.094 (\text{MoO}_3)^2 - 1.076 (\text{CoO})^2 - 0.061 (\text{WO}_3)^2 \\ & - 0.053 (\text{MoO}_3) (\text{WO}_3) \end{aligned}$$

The presence of MoO_3 , CoO , and WO_3 significantly affected the denitrogenation and the coefficients of quadratic and the interaction of the metal oxide concentrations were negative. The intercept at 37.43 was close to a denitrogenation value obtained with the blank carrier.

The weight percent desulfurization is plotted against the weight percent MoO_3 in Figure 24 ignoring the presence of CoO and WO_3 . The catalytic abilities of these same metals were also demonstrated in desulfurization. The correlations between the weight percent desulfurization and MoO_3 concentration are illustrated in Figure 25 at three different levels of CoO . Within each of these CoO levels, three levels of WO_3 concentrations were also considered. It is clearly seen from the figure that there is an optimum MoO_3 concentration (around 10%) in each group of curves. The effect of weight percent CoO is extremely significant when its concentration was increased from 2% to 4% but further increase beyond 4% actually deteriorated catalytic desulfurization activities. The effect of tungsten concentration in desulfurization was not so significant at all levels of MoO_3 and CoO . The desulfurization as a function of CoO is shown in Figure 26 and Figure 27. The cobalt exhibited a most distinctive enhancement effect in desulfurization with peaks around 4%. This trend was clearly visible at all three levels of MoO_3 concentrations. The sulfur removal as a function of WO_3 concentration is shown in Figure 28. The catalytic performance in desulfurization as a function of three metals are shown in Figure 29. The figure indicates that there are significant interactions.

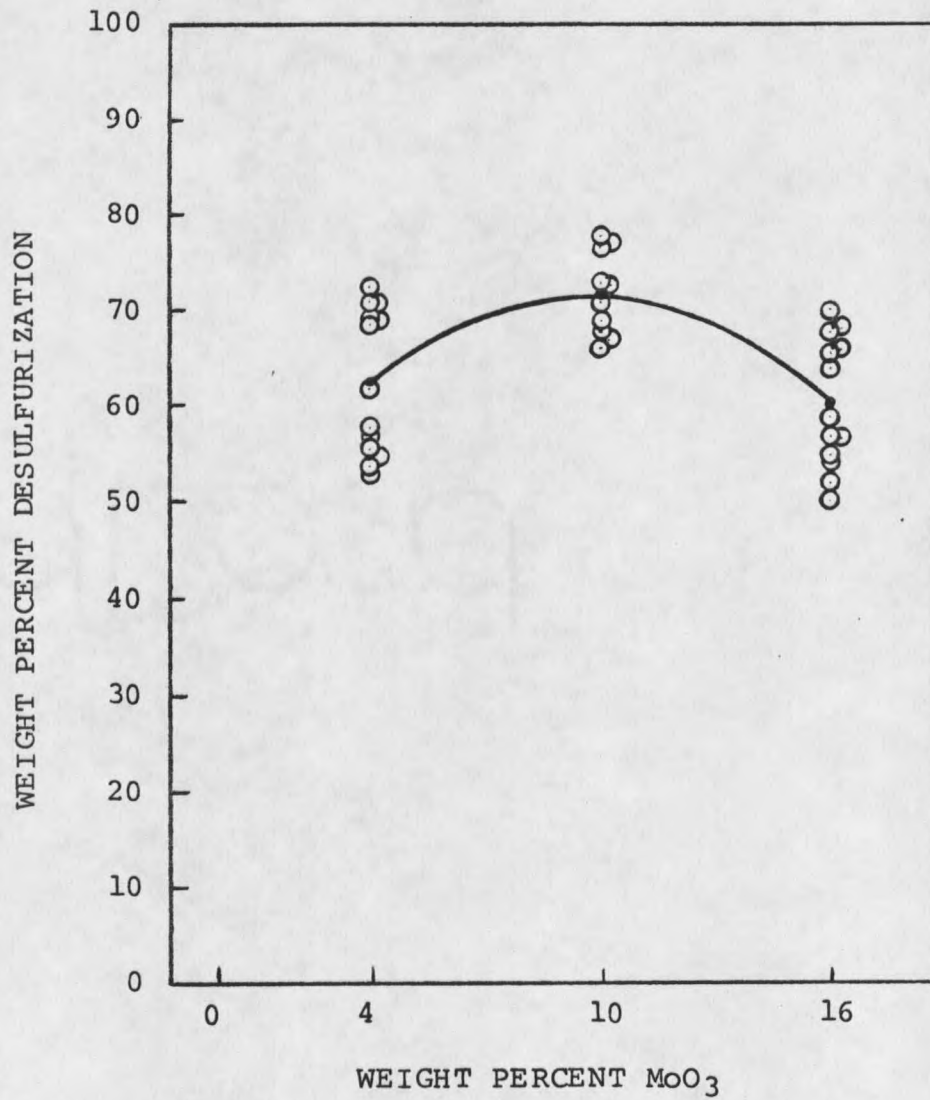


Figure 24. Catalytic performance in desulfurization as a function of MoO₃ concentration.

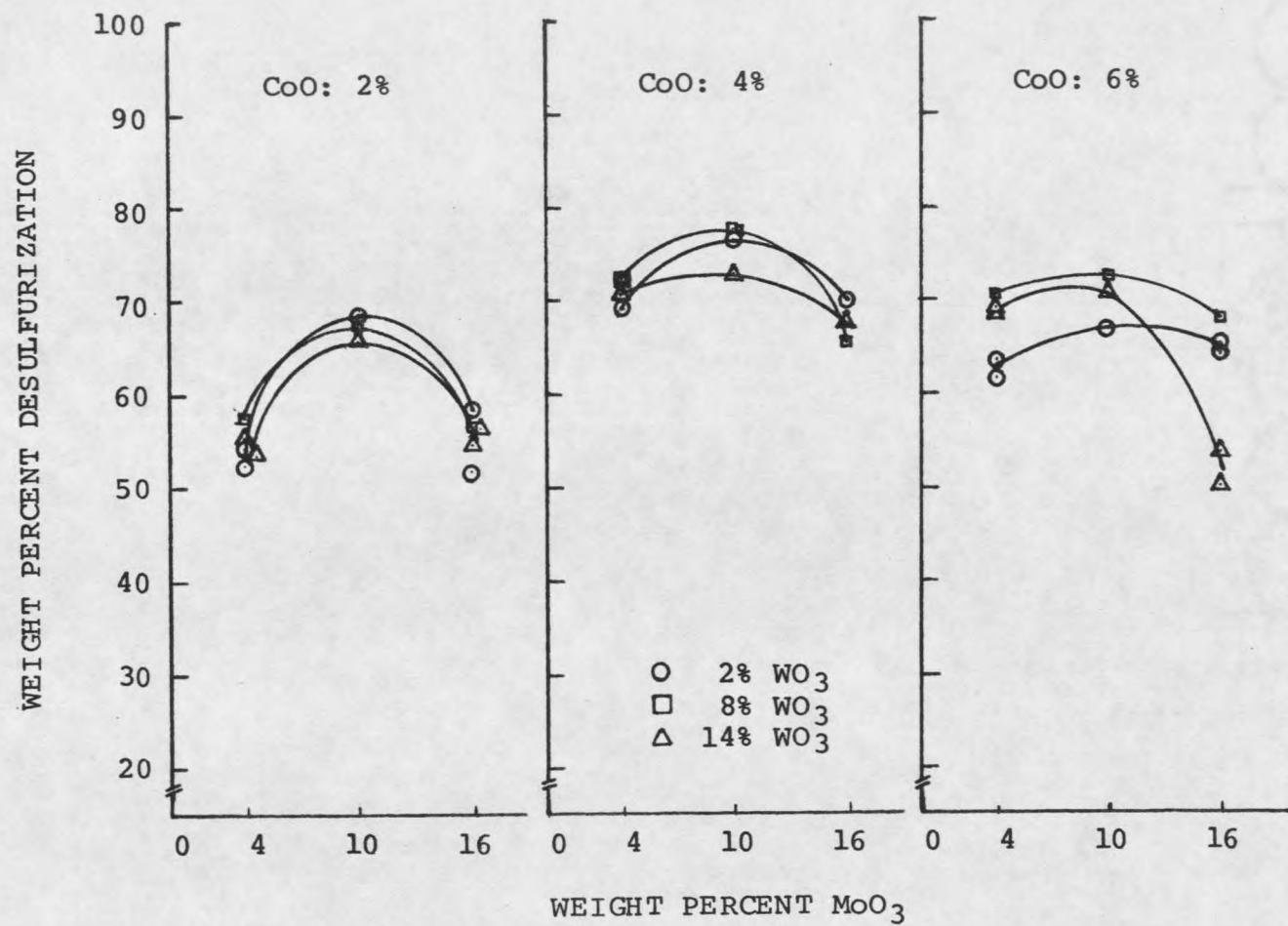


Figure 25. Catalytic performance in desulfurization as a function of CoO, WO₃, and MoO₃ concentrations.

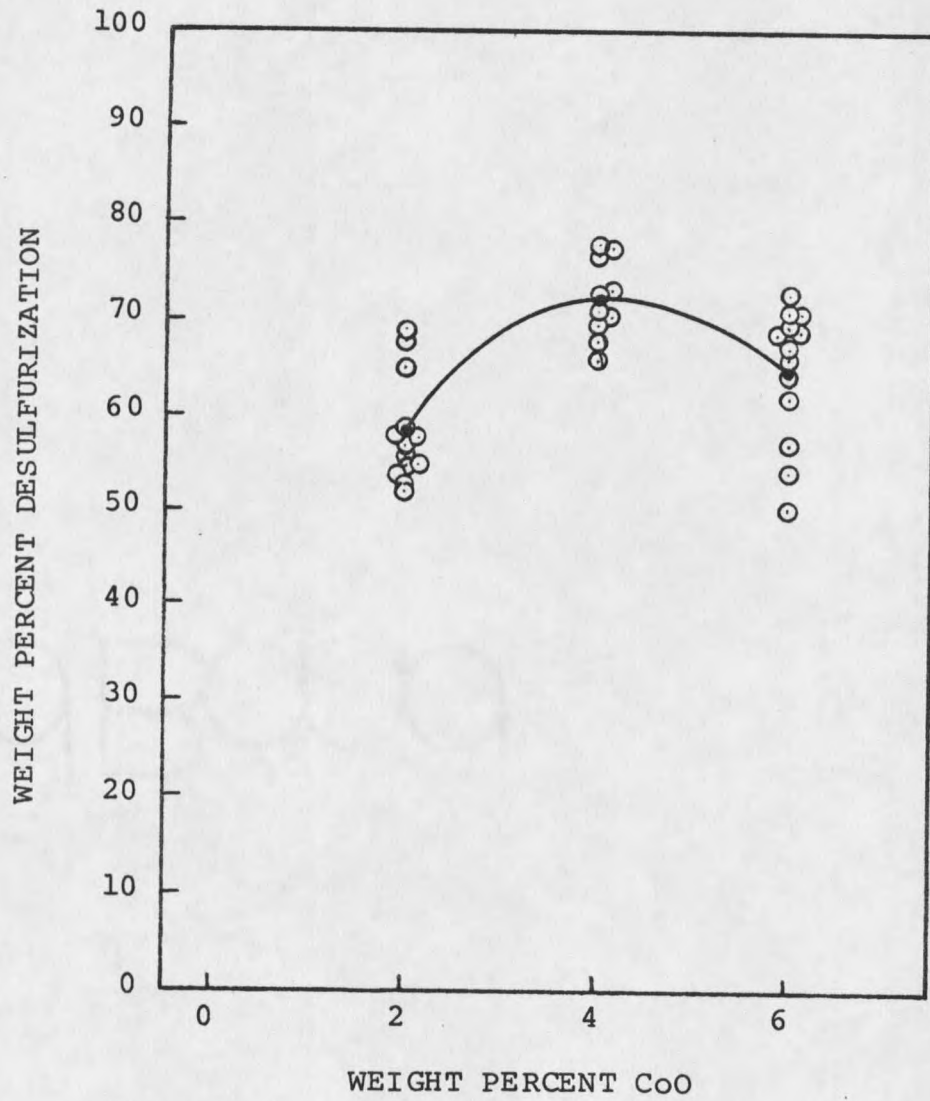


Figure 26. Catalytic performance in desulfurization as a function of CoO concentration.

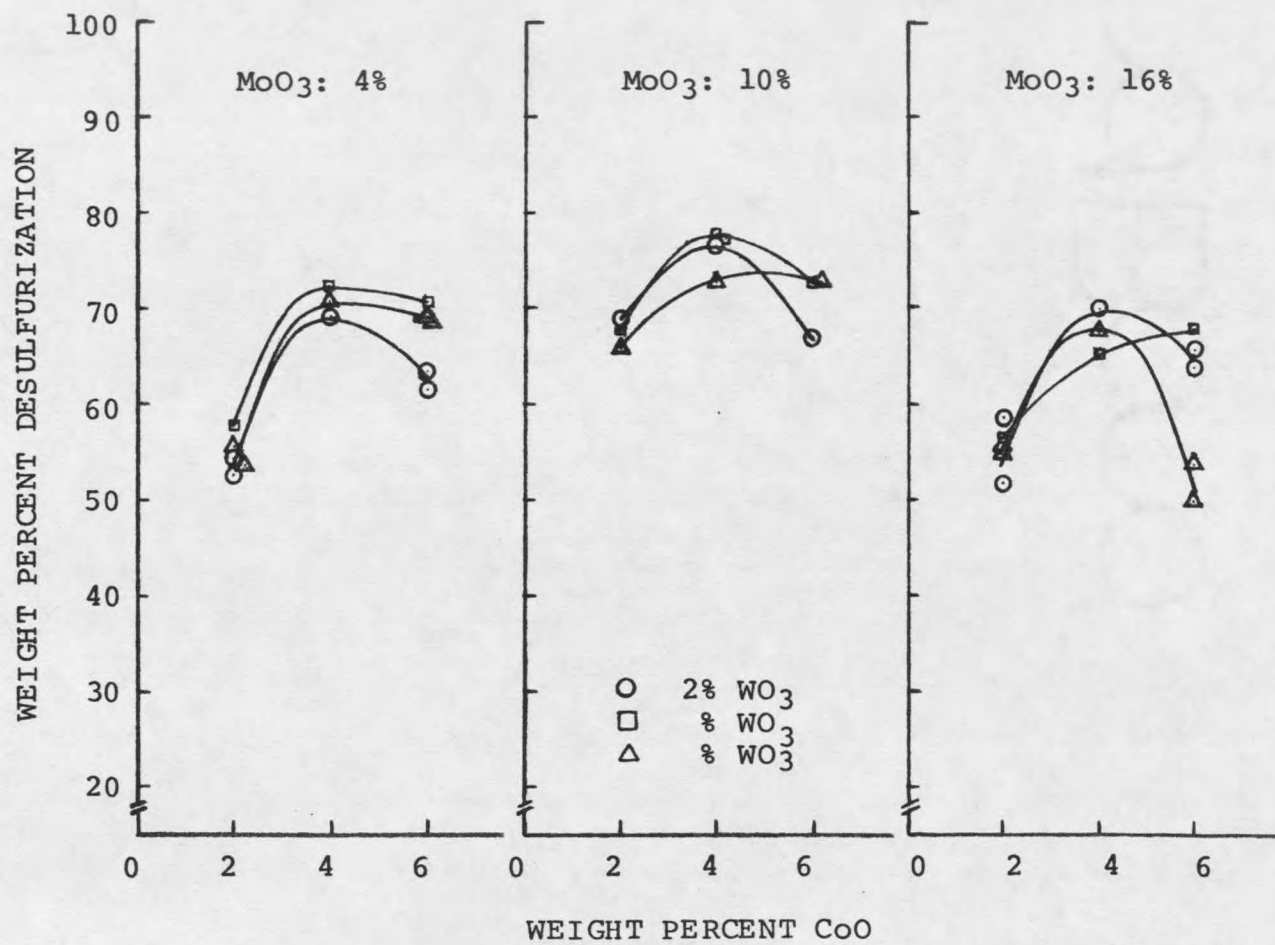


Figure 27. Catalytic performance in desulfurization as a function of MoO₃, WO₃, and CoO concentrations.

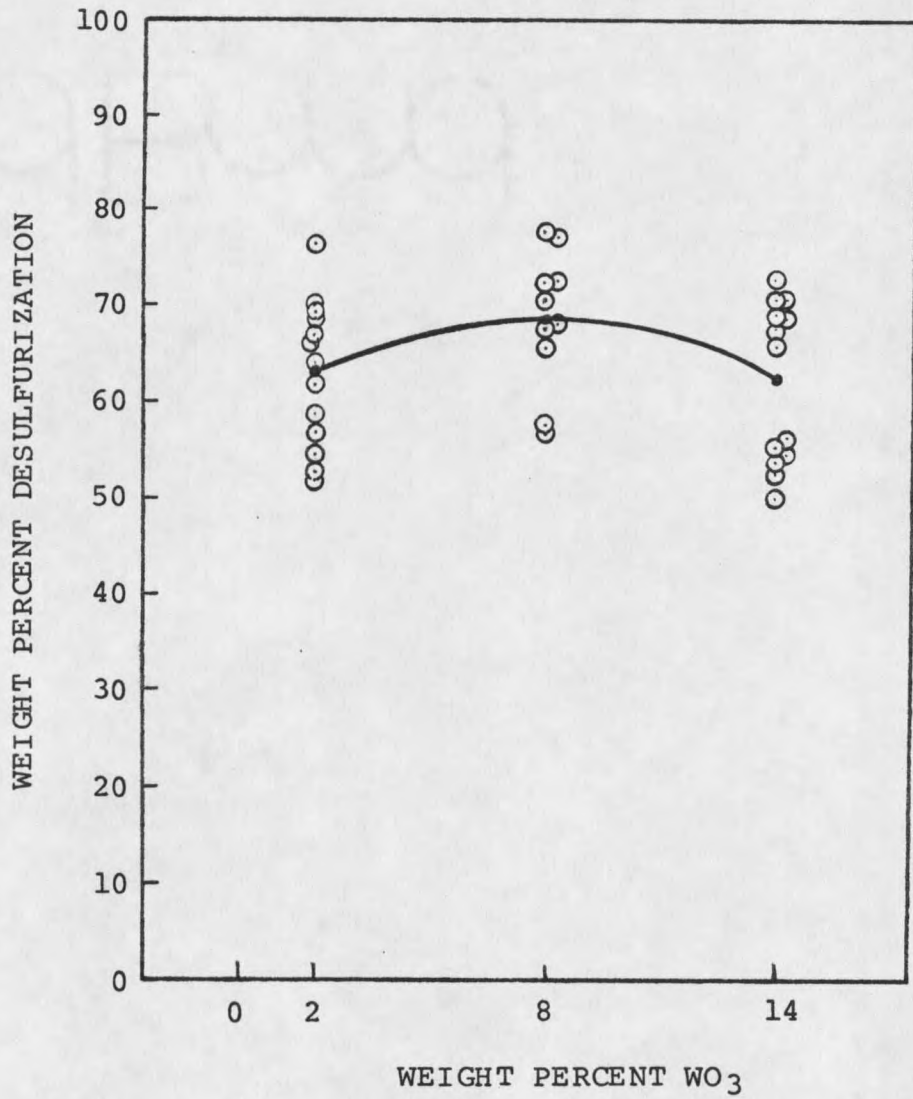


Figure 28. Catalytic performance in desulfurization as a function of WO_3 concentration.

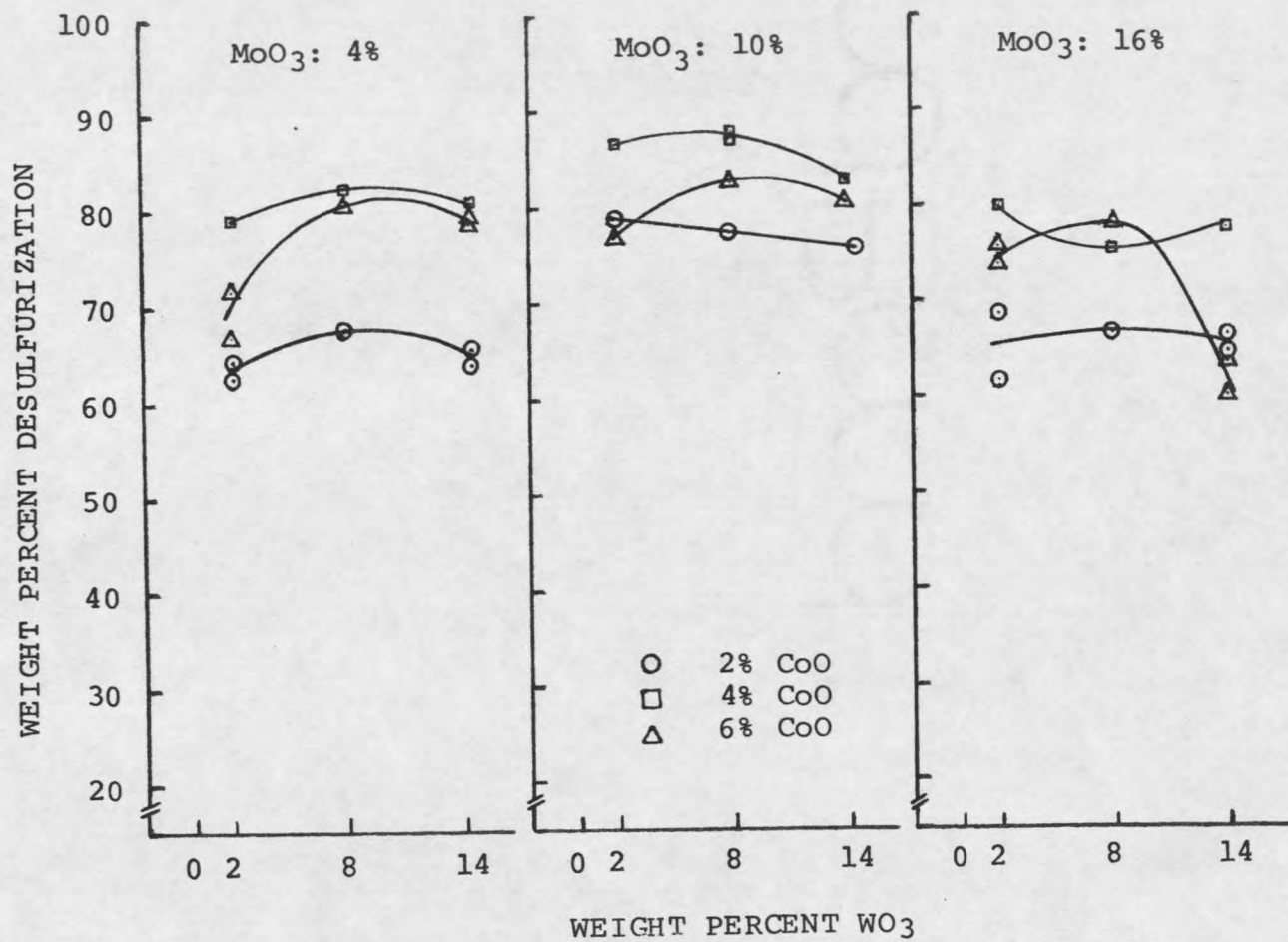


Figure 29. Catalytic performance in desulfurization as a function of MoO₃, CoO, and WO₃ concentrations.

An analysis of variance was made for data in the configuration of a response variable (desulfurization) with three classifying factors arranged in randomized complete block (Table XIV). An unweighed means procedure was also used here for unequal replications. Based on the F-value of the fifth column, the interaction between MoO_3 and CoO is the least significant. The use of backward stepwise approach produced a table of multiple linear regressions at a significance level of 5% (Table XV). The regression equation thus obtained is

$$\begin{aligned} \text{Wt\% DeS} = & 5.2 + 4.99 (\text{MoO}_3) + 19.14 (\text{CoO}) + 2.03 (\text{WO}_3) \\ & - 0.23 (\text{MoO}_3)^2 - 2.19 (\text{CoO})^2 - 0.086 (\text{WO}_3)^2 \\ & - 0.071 (\text{MoO}_3) (\text{WO}_3) \end{aligned}$$

The effect of the three metals on desulfurization was extremely significant. The quadratic and interaction effects of these metals were negative as in denitrogenation. The intercept at 5.2% was much the same as the desulfurization value of 4.5% obtained with the blank carrier.

The degree of hydrocracking of SRL, that is, upgrading of hydrogen content is expressed in terms of two parameters: the percentage of gasoline distilled up to 380°F , or 193°C (light liquid) and the percentage of residue remained in the pot at 450°F , or 232°C (heavy liquid). The volume percentages of light and heavy distillates are plotted as a function of MoO_3 concentration, as a function of CoO concentration, and as a function of WO_3 concentration in Figure 30, Figure 31, and Figure 32.

Although there are significant interactions, it is generally seen that the maximum amount of gasoline was produced at around 9% MoO_3 concentration. The effect of CoO concentration on gasoline production appears to be insignificant. The tungsten concentration, on the other hand, played a significant role when the MoO_3 concentration was as low as 4%. In this case, at all levels of CoO concentration the gasoline yield increase was almost proportional to the WO_3 concentration (Figure 32). At higher MoO_3 concen-

Table XIV

Analysis of Variance for Desulfurization
as Response Variable

FACTOR = 1
 TRT N MEANS
 4 9 63.93
 10 9 70.92
 16 9 61.59

FACTOR = 2
 TRT N MEANS
 2 9 59.34
 4 9 71.22
 6 9 65.88

FACTOR = 3
 TRT N MEANS
 2 9 64.84
 8 9 67.45
 14 9 64.16
 HARMONIC CT= 1.200

ANALYSIS OF VARIANCE:

SOURCE	DF	S.S.	M.S.	F-VALUE	P-VALUE
1	2	423.4	211.7	49.13	0.000
2	2	636.5	318.2	73.85	0.000
1 2	4	62.02	15.50	3.598	.5112E-01
3	2	54.41	27.21	6.314	.1923E-01
1 3	4	67.49	16.87	3.916	.4125E-01
2 3	4	45.04	11.26	2.613	.1064
1 2 3	8	114.6	14.33	3.325	.4622E-01
RESIDUAL	9	38.78	4.309		

Three Levels

Factor 1 = Wt% MoO ₃	4%	10%	16%
Factor 2 = Wt% CoO	2%	4%	6%
Factor 3 = Wt% WO ₃	2%	8%	14%

Response Variable = Wt% desulfurization

Table XV

Multiple Regression Analysis for Desulfurization

DEPENDENT VARIABLE = 5

INDEPENDENT VARIABLES= 1 2 3 12 13 14 17

FIT:	VAR	R-PART	B	SE(B)	T	P-VALUE
	1	.7630	4.989	.7987	6.247	0.000
	2	.7918	19.14	2.791	6.859	0.000
	3	.4999	2.034	.6658	3.054	.4908E-02
	12	-.7500	-.2307	.3845E-01	-6.000	0.000
	13	-.7670	-2.189	.3461	-6.325	0.000
	14	-.3903	-.8626E-01	.3845E-01	-2.243	.3298E-01
	17	-.5093	-.7056E-01	.2253E-01	-3.131	.4051E-02

INTERCEPT = 5.199
R-SQUARED = .8355

ANALYSIS OF VARIANCE:

SOURCE	DF	S.S.	M.S.	F-VALUE	P-VALUE
REGRESS	7	1872.	267.4	20.32	0.000
RESIDUAL	28	368.5	13.16		
TOTAL	35	2240.			

- 5 = Wt% desulfurization
1 = Wt% MoO₃
2 = Wt% CoO
3 = Wt% WO₃
12 = (Wt% MoO₃) (Wt% MoO₃)
13 = (Wt% CoO) (Wt% CoO)
14 = (Wt% WO₃) (Wt% WO₃)
17 = (Wt% MoO₃) (Wt% WO₃)

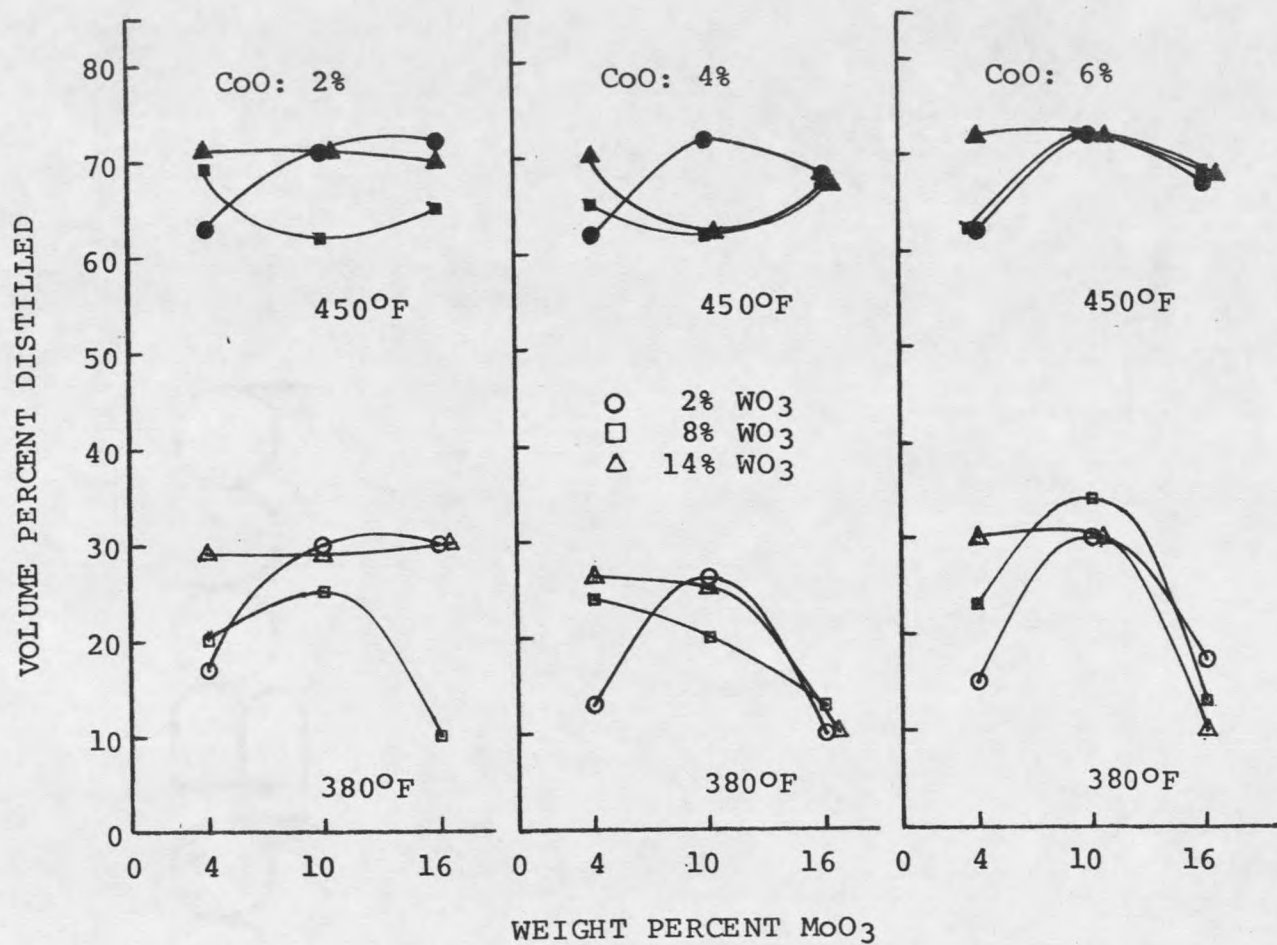


Figure 30. Catalytic performance in hydrocracking as a function of CoO, WO₃, and MoO₃ concentrations.

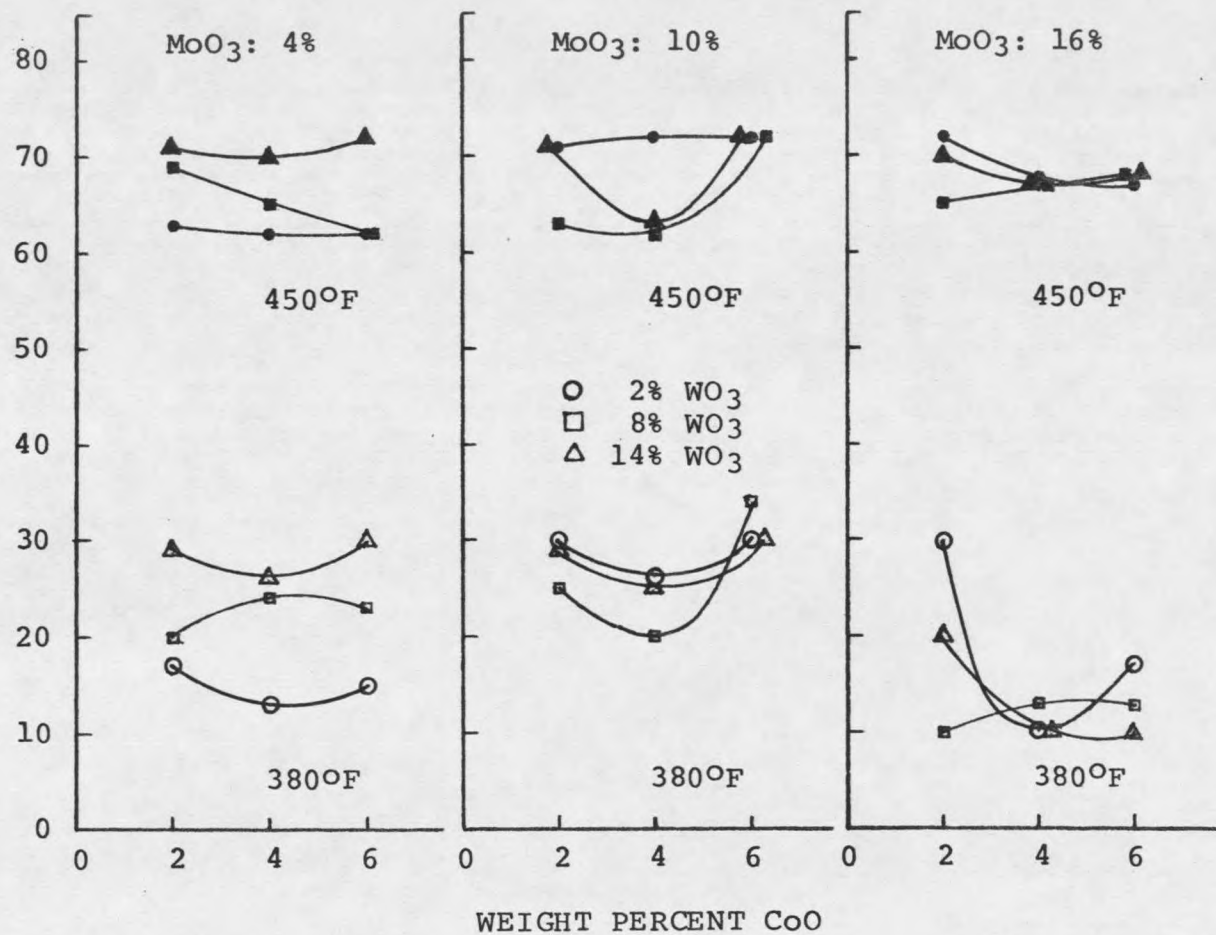


Figure 31. Catalytic performance in hydrocracking as a function of MoO₃, WO₃, and CoO concentrations.

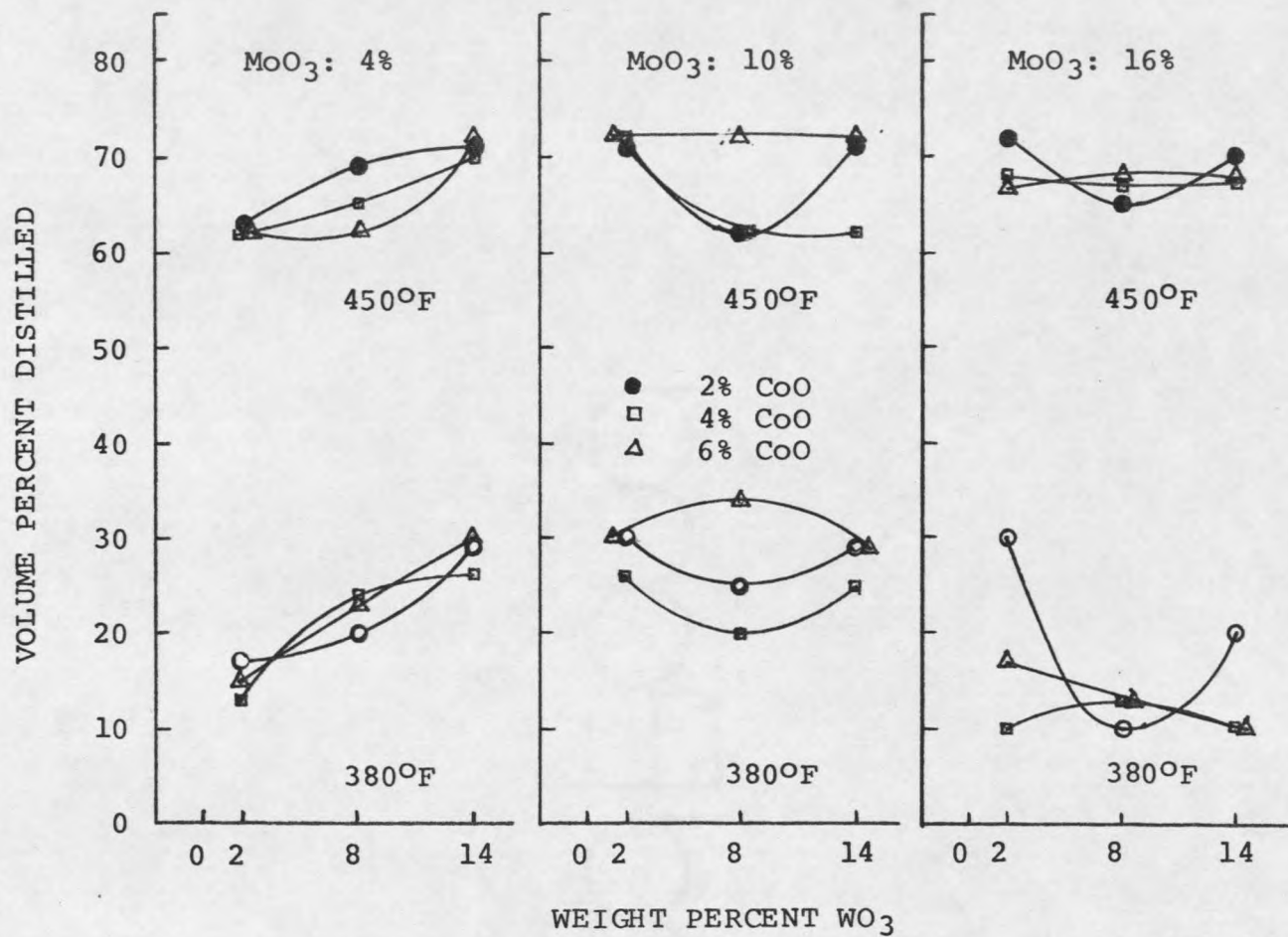


Figure 32. Catalytic performance in hydrocracking as a function of MoO₃, CoO, and WO₃ concentrations.

trations, this trend did not hold. An analysis of variance and a table of multiple linear regressions made for the response variable, volume percentage of gasoline produced, is shown in Table XVI and Table XVII.

Development of A Model for Catalyst

The Katalco carrier (serial no. 81-6731) was inspected under the scanning electron microscope. Figure 33 shows the scanning electron photomicrograph of catalyst surface at 50,000 times magnification. One millimeter in length in these figures is equivalent to 200Å (1Å = 1 ten-billionth of a meter). A base granule as small as about 80Å can be visually identified from the pictures. A summary of the granule size calculations is presented in Appendix D. The calculations show that the average size of a base granule is 74Å in diameter. Figure 34 shows one of the many possible models that can explain the physical properties of the catalyst carrier. It shows a highly organized pore structure with an average pore diameter of approximately 150Å in three dimensional coordinates. In reality, however, the pores are not well-defined cylindrical pores as evidenced by Figure 33.

Problems have been encountered in correlating the catalytic performance with a nominal pore diameter and surface area. A number of commercial catalysts, well-known for their denitrogenation capability with one type of feed, displayed poor performance with another type of feed [63,64]. It is believed that the nominal pore diameter as used in the monodisperse model is not an adequate parameter to represent a catalyst, particularly when the large molecular substance such as coal-derived liquid was treated.

Stenberg [62] reported that the SRL had an average molecular weight of 460 with a range of 160 to 4000 (gel permeation chromatographic separation). The SRL is highly aromatic with one acid group and 0.1 base group per molecule. The average thickness of the aromatic layers in the SRL samples is about 12Å, a stack of 4 planes with 15Å in diameter (powder X-ray diffraction).

Table XVI

Multiple Regression Analysis for Gasoline Yield

DEPENDENT VARIABLE = 6
 INDEPENDENT VARIABLES= 1 2 12 13

FIT:	VAR	R-PART	B	SE(B)	T	P-VALUE
	1	.5245	4.279	1.248	3.430	.1729E-02
	2	-.3959	-10.74	4.476	-2.400	.2258E-01
	12	-.5714	-.2390	.6164E-01	-3.877	0.000
	13	.3792	1.266	.5548	2.282	.2953E-01

INTERCEPT = 27.68
 R-SQUARED = .4529

ANALYSIS OF VARIANCE:

SOURCE	DF	S.S.	M.S.	F-VALUE	P-VALUE
REGRESS	4	886.6	221.7	6.416	.9504E-03
RESIDUAL	31	1071.	34.55		
TOTAL	35	1958.			

6 = Volume % gasoline yield

1 = Wt% MoO₃

2 = Wt% CoO

12 = (Wt% MoO₃) (Wt% MoO₃)

13 = (Wt% CoO) (Wt% CoO)

Table XVII

Multiple Regression Analysis for Heavy Oil Yield

DEPENDENT VARIABLE = 7

INDEPENDENT VARIABLES = 1 2 13 14 17

FIT:	VAR	R-PART	B	SE(B)	T	P-VALUE
	1	-.6076	-.7105	.1696	-4.190	0.000
	2	.3443	4.494	2.238	2.008	.5368E-01
	13	-.3390	-.5474	.2773	-1.974	.5769E-01
	14	-.6474	-.5602E-01	.1204E-01	-4.653	0.000
	17	.5860	.6878E-01	.1737E-01	3.961	0.000

INTERCEPT = 31.48

R-SQUARED = .4981

ANALYSIS OF VARIANCE:

SOURCE	DF	S.S.	M.S.	F-VALUE	P-VALUE
REGRESS	5	263.5	52.70	5.955	.8484E-03
RESIDUAL	30	265.5	8.849		
TOTAL	35	529.0			

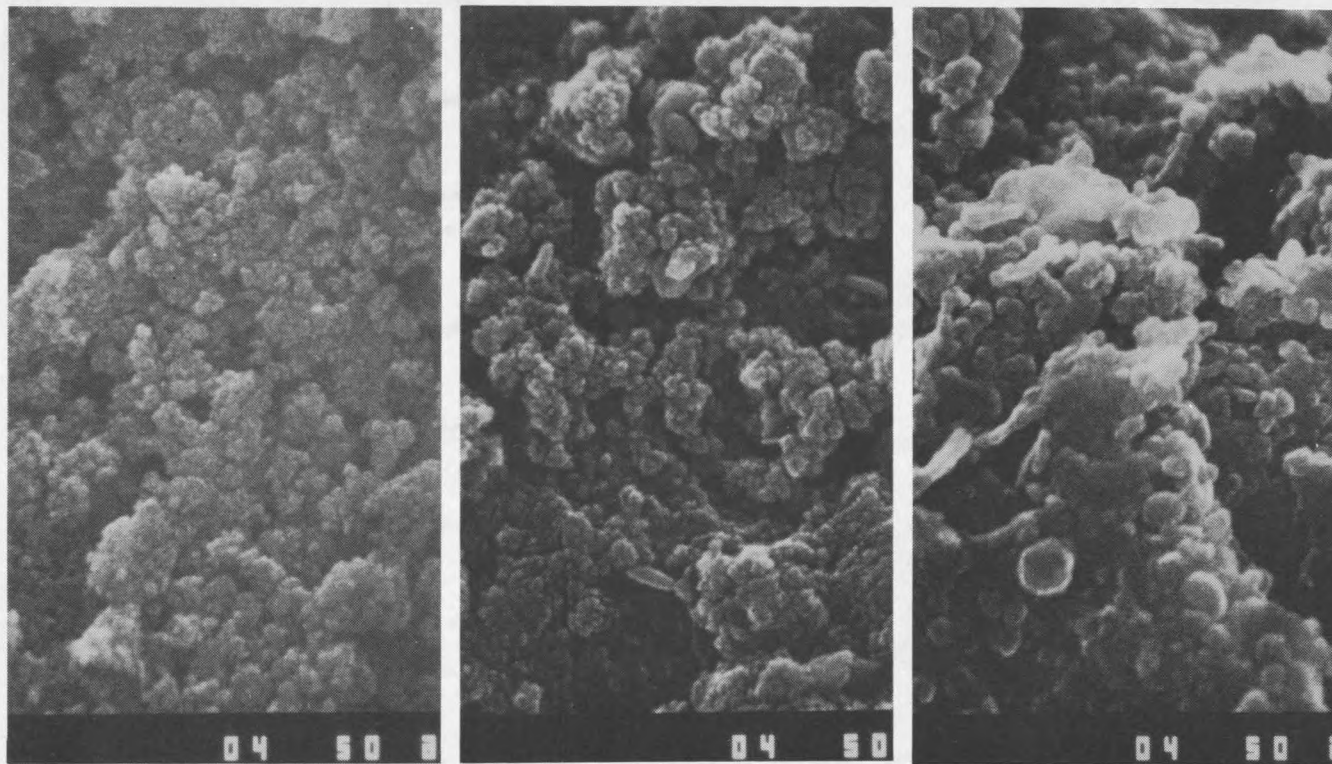
7 = Volume % heavy oil yield

1 = Wt% MoO₃

2 = Wt% CoO

13 = (Wt% CoO)**2

14 = (Wt% WO₃)**217 = (Wt% MoO₃) (Wt%WO₃)



(A)

(B)

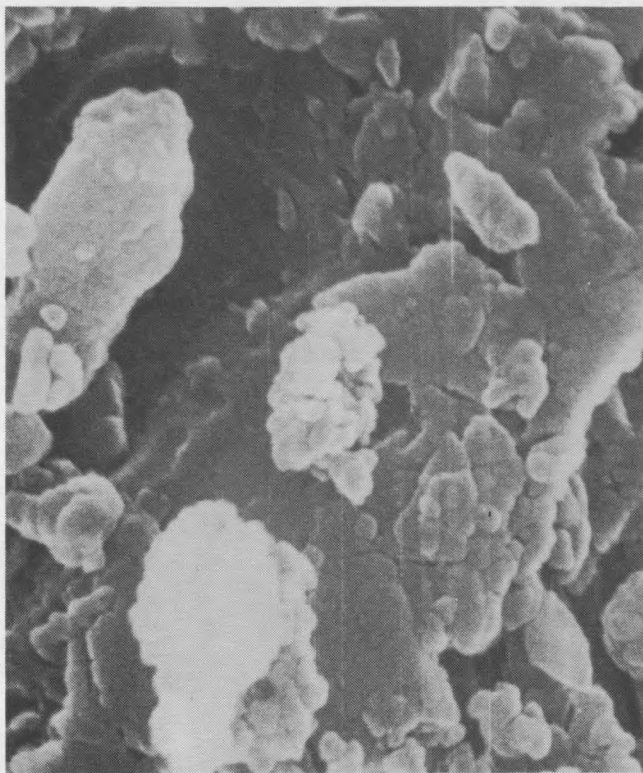
(C)

Figure 33. Scanning electron photomicrographs of various catalysts:

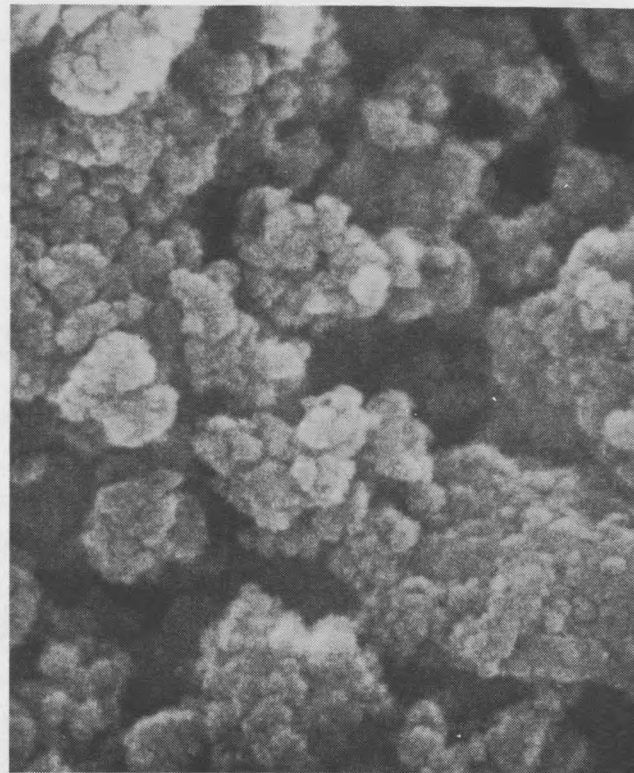
(A) Katalco blank carrier

(B) KT-14 with 10% MoO_3 , 4% CoO , and 8% WO_3 on Katalco carrier

(C) KT-14 after 8-hr run



(D)



(E)

Figure 33. (cont.)

(D) Union Carbide Linde 13X with 10% MoO_3 , 4% CoO , and 8% WO_3

(E) Ketjen LA-3P with 10% MoO_3 , 4% CoO , and 8% WO_3

